Kamila Kappke Dias
Bachelor degree in Biotechnology

Safety Assessment of Polymeric Nanoparticle Carriers for Drug Delivery in Human Osteoblasts

Dissertation to obtain the Master Degree in
Biochemistry for Health

Supervisor: Professor Maria João Silva, PhD, Instituto Nacional de Saúde Doutor Ricardo Jorge, Lisboa
Co-Supervisor: Professor Ana Bettencourt, PhD, Faculdade de Farmácia, Universidade de Lisboa

March, 2017

Kamila Kappke Dias
Bachelor degree in Biotechnology

Safety Assessment of Polymeric Nanoparticle Carriers for Drug Delivery in Human Osteoblasts

Dissertation to obtain the Master Degree in
Biochemistry for Health

Supervisor: Professor Maria João Silva, PhD, Instituto Nacional de Saúde Doutor Ricardo Jorge, Lisboa
Co-Supervisor: Professor Ana Bettencourt, PhD, Faculdade de Farmácia, Universidade de Lisboa

Jury:

President: Professor Maria Teresa Nunes Mangas Catarino, PhD, FCT-UNL

Argue: Elisabete de Jesus Oliveira Marques, PhD, FCT-UNL

Supervisor: Professor Maria João Silva, PhD, Instituto Nacional de Saúde Doutor Ricardo Jorge, Lisboa

March, 2017

Copyright

“Safety Assessment of Polymeric Nanoparticle Carriers for Drug Delivery in Human Osteoblasts”

“I would rather have questions that can’t be answered that answers which can’t be questioned”

Richard Feynman – Father of Nanotechnology

Acknowledgments

First of all, I would like to thank to my mentors Doctor Maria João Silva from Departamento de Genética Humana – Instituto Nacional de Saúde Dr. Ricardo Jorge and Doctor Ana Bettencourt from Faculdade de Farmácia, Universidade de Lisboa, that allowed me to work their laboratories, for all the guidance, the support, the knowledge and for always being available to discuss my crazy ideas. Without them, none of this would be possible.

To my non-official mentors, Doctor Henriqueta Louro and Doctor Lídia Gonçalves, for all the teaching, the limitless patience and for making feel welcome all the time.

To both institutions, *Insituto Nacional de Saúde Dr. Ricardo Jorge and Faculdade de Farmácia da Universidade de Lisboa* who gave me the opportunity to perform this study, for the accommodation and technical support along this project.

I also want to show my gratitude to all my lab colleagues for all the help and the fun moments, specially Célia Ventura, for all the laughs, the friendship and the support.

To all friends from Coimbra and Lisboa for their fellowship, and for making this journey way better than it was.

Lastly, to my family, specially to my mom, for her support and affection, and to Tiago, for always being right by side and for never stop encouraging me.

Thank you all for believing in me!

Abstract

Nanoparticles (NPs) applied to pharmaceutics constitute an innovative approach to improve drug release profiles on targeted sites. The assessment of their biocompatibility and safety for human health plays also a major role in the development process. The objective of this work was to characterize the cellular interactions and potential toxicity of polymeric nanoparticles, in human osteoblasts.

Poly(methyl methacrylate) (PMMA) and Eudragit® RL 100 (Eud) were used to produce PMMA and PMMA-Eud (50:50) NPs (average size range of 500 nm) by single-emulsion with solvent evaporation methodology. Their physicochemical properties (size distribution, surface charge, morphology and aggregation/agglomeration states) were analysed. Their safety evaluation was conducted in "normal" and differentiated MG63 cells. Cell uptake, cyto- and genotoxicity were characterized using several endpoints: cell viability (MTT assay), oxidative stress production (H_2DCFDA assay), DNA and chromosome damage (Comet and Micronucleus assays).

The results confirmed the successful cellular uptake of PMMA and PMMA-Eud. Both NPs were neither cytotoxic nor able to produce oxidative stress in differentiated cells, although a moderated toxicity was detected in undifferentiated cells. As to the genotoxic potential, both NPs induced primary DNA damage (comet assay) in osteoblasts, especially in short-term exposure. Noteworthy, none of the NPs caused chromosome alterations, indicating that the DNA lesions were not converted into permanent genetic damage. However, an increased cell proliferative capacity was noted for PMMA that needs confirmation.

In conclusion, PMMA and PMMA-Eud are promising nanocarriers in drug delivery systems. Their in vitro safety assessment in osteoblasts indicated that both NPs are biocompatible but display a weak genotoxicity that needs further investigation, e.g., using other endpoints or in vivo models. The utilization of cells under different specialization status improved data reliability. Moreover, understanding how physicochemical features relate to toxicity will support the design of safer formulations for biomedical purposes as envisaged by the safer-by-design concept.

Key-words: nanocarriers, PMMA, PMMA-Eud, safety evaluation, nanotoxicology, osteoblasts.

Resumo

A aplicação de nanopartículas (NPs) à área farmacêutica constitui uma resposta inovadora para melhorar os perfis de libertação de fármacos em órgãos-alvo. No entanto, a avaliação da sua biocompatibilidade e segurança para a saúde humana constituem uma fase limitante. O objetivo deste trabalho foi caracterizar o potencial tóxico de NPs poliméricas e possíveis interações com osteoblastos de origem humana.

Foi utilizado poli(metil metacrilato) (PMMA) e Eudragit® RL 100 (Eud) para a produção das NPs (tamanho médio: 500nm), através do método de emulsão simples com evaporação do solvente. Seguiu-se uma caracterização das suas propriedades físico-química incluindo a distribuição de tamanhos, carga superficial, morfologia e formação de agregados/aglomerados. A avaliação de segurança foi realizada em células "normais" e diferenciadas de osteoblastos (MG-63). Foi analisada a capacidade de internalização destas NPs assim com a sua cito- e genotoxicidade através de vários parâmetros: viabilidade celular (ensaio do MTT), stress oxidativo (ensaio do H_2DCFDA) e danos ao nível do DNA e da estrutura cromossómica (ensaios do Cometa e dos Micronúcleos).

Os resultados confirmaram uma internalização bem-sucedida tanto para o PMMA como para o PMMA-Eud. Ambas as NPs não demonstraram citotoxicidade nem capacidade de induzir stress oxidativo em células diferenciadas, apesar de uma toxicidade moderada ter sido detetada em células indiferenciadas. Quanto ao potencial genotóxico, ambas as NPs induziram danos primários ao nível do DNA, especialmente em exposições mais curtas. Nenhuma NP causou alterações cromossômicas, indicando que as lesões induzidas ao DNA não foram convertidas em danos genéticos permanentes. No entanto, foi observado um aumento da capacidade proliferativa das células quando expostas a NPs de PMMA que ainda necessitam de confirmação.

Em conclusão, o PMMA e o PMMA-Eud apresentam propriedades distintas para uma aplicação na veiculação de fármacos. A sua avaliação de segurança *in vitro* em osteoblastos indicou que ambas as NPs são biocompatíveis, mas apresentam uma genotoxicidade moderada que necessita de ser explorada, através de outros parâmetros ou modelos *in vivo*. A utilização de células sob diferentes estados de especialização aumentou a sensibilidade dos ensaios. Além disso, compreender a relação entre as características físico-químicas e uma potencial toxicidade irá promover a produção de formulações mais seguras para fins biomédicos como previsto pelo conceito "*safe-by-design*".

Palavras-chave: nanopartículas, PMMA, PMMA-Eud, avaliação de segurança, nanotoxicologia, osteoblastos

Table of Contents

Table of Figures

List of Tables

List of Acronyms and Abbreviations

Abbreviation	Meaning
ATCC	American Type Culture Collection
AP	Alkaline Phosphatase
BCA	Bicinchoninic Acid
BNC	Binucleated Cell(s)
BSA	Bovine Serum Albumin
CBMN	Cytokinesis-Block Micronucleus
CBPI	Cytokinesis-Block Proliferation Index
Cyt-B	Cytochalasin-B
DCM	Dichloromethane
DMSO	Dimethyl Sulfoxide
EDTA	Ethylenediamine Tetraacetic Acid
Eud	Eudragit® RL 100
EMS	Ethyl Methanesulfonate
FDA	Food and Drug Administration
FPG	Formamido-Pyrimidine-DNA-Glycosilase
ICH	International Council for Harmonisation
ISO	International Organization for Standardization
LDV	Laser Doppler Velocimetry
LD	Laser Diffraction
H_2DCFDA	2-7' dichlorodihydrofluorescein diacetate
MMA	Methylmethacrylate
MMC	Mitomycin C
MNi	Micronucleus
MNBNC	Micronucleated Binucleated cell(s)
MRSA	Methicillin Resistant *Staphylococcus aureus*
MTT	[3-(4,5-dimethylthiazol-2-yl)-2,5-diphenyltetrazolium bromide]
NB	Nuclear Bud
NM	Nanomaterial
NP	Nanoparticle
NPB	Nucleoplasmatic Bridges
OD	Optical Density
OECD	Organisation for Economic Co-operation and Development
PBS	Phosphate Buffered Saline
PMMA	Poly(methyl methacrylate)
PVA	Poly(vinyl alcohol)
PEG	Polyethylene glycol

RI	Replicative Index
RPMI	Roswell Park Memorial Institute
SB	Strand Breaks
SD	Standard Deviation
QSAR	Quantitative Structure Activity Relationship
RANK	Receptor Activator for Nuclear Factor K
RANKL	Receptor Activator for Nuclear Factor K Ligand
RFU	Relative Fluorescence Units
ROS	Reactive Oxygen Species
RT	Room Temperature
SEM	Scanning Electron Microscopy
SESE	Single Emulsion Solvent Evaporation
SDS	Sodium Dodecyl Sulfate
TB	Trypan Blue
VRSA	Vancomycin Resistant *Staphylococcus aureus*

1. Introduction

1.1 Nanoparticles and Nanotechnologies

The rapid expansion of nanotechnology has been widely spread in our society and becoming increasingly important in multiple areas of interest not only in the medicine and pharmacology, but also in food industry (packing and additives), cosmetics, eletronical devices, paints, clothing, etc (Arora et al. 2012). Different consumer products with nanoparticles (NPs) in their composition are available and daily consumed. When Richard Feynman faced the nanoscale (10^{-9} m), he also discovered new properties and functions from common chemical elements not described for classical laws of physics (Sanchez & Sobolev 2010). NPs present size-dependent properties. Their surface-volume ratio comprises a higher percentage of surface atoms leading to reactive materials that tend to interact with other molecules (Klabunde 2009). Besides the high reactivity, NPs also present particular physicochemical features, including electrical conductivity, optical and magnetic properties that render them very attractive for multiple industrial and biomedical applications.

One of the controversies around nanotechnology is the definition of nanomaterial (NM). The European Commission published a specific recommendation (2011/696/EU) proposing a definition for nanomaterial where 50% or more particles (in an unbound, aggregate or an agglomerate state) belongs to a distribution range between 1-100nm (Rauscher et al. 2015). However, the nanoscale is also the scale at which properties of materials are different than they are at the macro or microscale, although this characteristic is not comprised in the definition. For this reason, in nanomedicine, it also include particles up to 1000 nm, regarding potential materials with new medical applications (Wagner et al. 2006).

Among the above mentioned as distinct and valuable properties of nanomaterials, nanomedicine has emerged with the intention of adopting these materials for medical diagnosis or therapeutics to improve health strategies. In fact, the ability of NPs to cross biological barriers can provide applications in drug delivery, imaging and diagnostic, therapies and novel of drug discovery (Wagner et al. 2006). Among all this diverse world that is encompassed by the nanomedicine, an approach for solving osteomyelitic infections and further problems associated with conventional treatments is expected to emerge.

1.2 Bone grafts and Osteomyelitis: A challenge to find new therapeutic approaches

1.2.1 Bone structure and formation

Bone is a complex and mineralized form of connective tissue that provides mechanical support to the whole body (Murugan & Ramakrishna 2005). With the ability of self-regeneration and self-remodelling during lifetime, bones are a well-protected organ remotely predisposed to infections and fractures (Grabowski 2015). Osteogenesis can be accomplished by intramembranous ossification or by endochondral ossification. The first one is assigned to the development of craniofacial bones and the second is responsible for the other structures present in the body (Gilbert 2000).

The endochondral ossification is conducted by multiple and synchronized actions performed by different cell types (Gilbert 2000). Bone formation begins with mesenchymal cells condensation and posterior differentiation into chondrocytes that are cells able to form cartilaginous tissue. Chondrocytes proliferate until they become hypertrophic and apoptosis events are induced (Clarke 2008). This gap allows vascularization and the influx of osteoblasts. These cells mediate bone matrix formation and mineralization, leading to a complete replacement of cartilage by bone. Bone resorption is carried out by osteoclasts, another important constituent of bone (Grabowski 2015). Bone is described as a dynamic tissue because is constantly being resorbed by osteoclasts and replaced by osteoblasts, thus assuring bone remodelling (Ducy et al. 2000).

1.2.2 Bone grafts

In spite of bone being a well-protected organ of our body, it is still prone to degeneration, pathology and trauma that may lead to the destruction of bone integrity. This tissue has the ability of self-regeneration, but this feature also tends to be reduced by age and cumulative injuries. Thus, external intervention is often required. Murugan et. al (2005) reports 550.000 cases of surgical interventions related to bone grafting per year in U.S.A. and it tends to increase. Bone grafting can be defined as a replacement of the damaged area and restoring of bone volume and structure (Bagherifard 2017). There are different ways to perform bone grafts: it can be autologous, allograft or synthetic. Autologous grafts are associated with the use of bone from the same individual. Usually, it is harvested from non-essential zones such the iliac crest or Gerdy's tubercle (tibia). Allografts are similar to autografts, but the bone material is removed from another patient. It can be harvested or donated by bone/tissue banks (Finkemeier 2002). Synthetic grafts are related to the development of manufactured materials that can mimic bone architecture and functions without harmful effects (Gong et al. 2015)

Autografts and allografts are regularly surgeon's first choice. It happens because these types of inserts are easily re-vascularized and well-accepted by the body (Finkemeier 2002). The grafts are also osteoinductive and osteogenic, which is essential to regenerate the lost bone and recover its normal activity. However, these procedures present further problems leading to donor site morbidity, excessive inflammation, pathogen transfer (allografts), among others (Bagherifard 2017). A statistical study has shown rates between 9 and 21% of major and minor complications associated with autologous bone grafts (Finkemeier 2002). Besides that, surgical procedures represent a huge obstacle as well.

The search of synthetic materials that enable bone regeneration has dramatically increased over the last years. This search has included not only the creation or adaption of bio-inert materials, but also the introduction of bioactive compounds to integrate and regenerate the lost tissue. Despite being a broad field of interest, the most used biomaterials are bioactive ceramics or glasses, biological and synthetic polymers. Hydroxyapatite-based material, hydrogels (e.g. polyethylene glycol), bioactive glasses with Ca^{2+}, polylactide, polyglycolide, poly(methyl methacrylate) and polyesters are just a few examples of a very extended list of the available materials that can be used in orthopaedic implants (Stevens 2008; Yu et al. 2015)

However, surgical interventions and medical devices implantation, promote an imbalance of the immune system. This can lead to pathogenic organisms' migration to the body leading to infection development, secondary to surgeries and orthopaedic implants.

1.2.3 Bone infections: Osteomyelitis

Among pathogenic microorganisms, *Staphylococcus aureus* and *Staphylococcus epidermidis* are by far the most commonly involved in joint infections. Usually, bone and joint infections associated to these bacteria are defined as osteomyelitis. This condition generally results in bone destruction and necrosis, and the spread of inflammation to other regions (Birt et al. 2017). When bacteria competently enter in the host tissue and are able to reproduce, they induce an acute inflammatory reaction. *S. aureus* expresses on their surface adhesins (e.g. laminin and fibronectin) that promote attachment to the host (Foster 1996). The specific receptor that promotes adherence to collagen is particularly associated with strains that cause osteomyelitis and septic arthritis.

S. aureus and *S. epidermidis* also have a predisposition to form biofilms on medical devices. Biofilms represent a complex group of microbial cells that adhere and colonize the surfaces representing a serious problem not only for the patient but also a public health issue (Donlan 2001). A better understanding of biofilm formation mechanism can provide new perspectives of successful treatments. As shown in figure 1, this process comprises different stages: the first one starts with the adhesion of free bacteria on the medical device. They start to proliferate and interact with the surface. That unrestrained proliferation leads to the micro-colony

formation and posterior stabilization. A cumulative cell grow, leads to the production of several layers on the prosthetic surface. Polysaccharides are produced as well, forming a barrier to protect microbes and enabling a matured biofilm. A significant decline on nutrients is experienced, so bacterial cells disperse from the mature film and enter into the bloodstream spreading the infection to other tissues (Veerachamy et al. 2014).

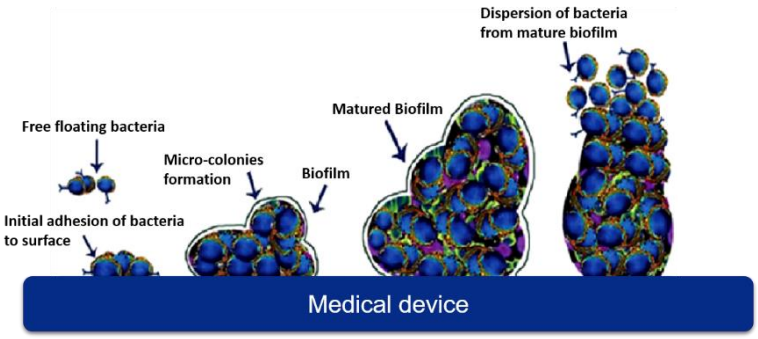

Figure 1: Biofilm formation process on a medical device. Adapted from Veerachamy et al. 2014

In a dense cell assembly, it is also expressed an altered phenotype, gene expression and protein production. This strongly reduces the chances of eradicating the infection. For this reason, an early and accurate diagnosis can help to decrease the spread of the disease. The diagnostic procedures used in osteomyelitis often requires bone biopsy. After that, cell culture of infected bone, peripheral blood cell counts, erythrocytes sedimentation rates and serum protein C-reactive are analysed and are usually increased if the patient experienced osteomyelitis (Lew & Waldvogel 2004). However, different studies revealed variations on these markers, appearing increased or decreased due to other infections, as the initial or advanced stages of the infection also affect the results (Davis 2005). Imaging methods also play a major role in diagnosing skeletal infections. Radiography, for example, can assess soft tissues, narrow joint spaces and bone destruction. But between 10-21 days of infection, bone destruction is still not clear. Other different imaging techniques with high power resolution are able to perform an accurate diagnosis. A computed tomography or a magnetic resonance imaging using radiopharmaceuticals may present very detailed results (Lew & Waldvogel 2004). The major drawback associated with these processes are the high costs, making them not generally available for the entire population.

Treatments associated with osteomyelitis are essentially based on antibiotics use. A combined antimicrobial and surgical procedure are usually considered when osteomyelitis reach an advanced stage (chronic osteomyelitis) (Davis 2005). Diagnosis already represents an obstacle and choosing adequate antibiotics may represent another problem. The approach tends to use a two-drug combination trying to cover the most recurrent microorganisms in bone infections. Long and invasive administrations represent high costs and further complications associated with intravenous catheters and systemic toxicity. Moreover, the increased prevalence

of Methicillin-resistant *S. aureus* (MRSA) and Vancomycin-resistant *S. aureus* (VRSA) strains has been reducing the prospect of infection eradication (Lew & Waldvogel 2004). Other antibiotics, such daptomycin, have shown interest results regarding fewer side effects for the patient and active penetration in biofilms, another significant barrier to antimicrobial agents (Mascio et al. 2007).

With the present alternatives, osteomyelitis still represents a great financial burden and reduces life quality for patients. New diagnose, and treatments are essential to overcome these problems and to assure improvement in life expectancy.

1.3 Novel nanoparticles-based therapeutics for Osteomyelitis

Novel materials and formulation at the nanoscale are being developed to act like drug delivery-systems revealing great benefits. NPs are able to promote an effective delivery of high doses of a drug at target sites during larger periods of time and with reduced systemic toxicity(Bettencourt & Almeida 2014). In other words, it will regulate the biodistribution and enhance the therapeutic index of drugs. It may represent an appropriated option to eradicate the biofilm formation.

1.3.1 Polymeric nanocarriers for drug delivery

Polymeric NPs represent a milestone on the drug delivery field. This is due to their increased colloidal stability, good chemical resistance, and the easy surface functionalization. This nano-scaled drug delivery system can provide a controlled release and an efficient targeting process (Goldberg et al. 2011).

1.3.2 Nano-sized Poly(methyl methacrylate) and Eudragit formulations

Poly(methyl 2-methylprop-2-enoate) (IUPAC) or, more commonly, Poly(methyl methacrylate) (PMMA) is a synthetic and amorphous homopolymer of methylmethacrylate (MMA) monomer (Bettencourt & Almeida 2012). As presented in figure 2, PMMA is a building block of MMA monomers.

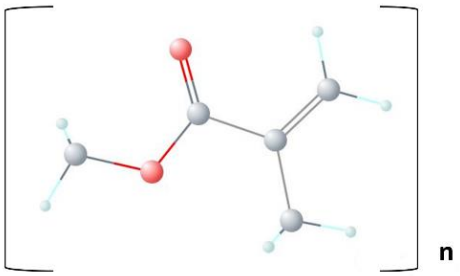

Figure 2: PMMA structure. In red are presented oxygen atoms and in blue are hydrogen atoms. Adapted from PubChem Compound Database; accessed on Feb. 3, 2017.

PMMA can also be described as a thermoplastic with glass transition temperature of 105ºC (Bettencourt & Almeida 2012). It is soluble in most organic solvents, but poorly soluble in water (50.5 mg/mL, at 25ºC). However as it comes in contact with water, the contact angle tends to decrease and the NPs become slightly hydrophilic (PubChem Compound Database; accessed on Feb. 3, 2017). Their polymerized form is found in many products, in multiple areas. Due to its optical properties, PMMA is often used as implantable intraocular and contact lenses, and even as a glass substitute (Santos et al. 2011). It also has applicability in dental and mandibular implants, but it is in orthopaedic surgery the most important appliance of PMMA. This polymer is often used as a bone cement for total hip replacement or for other joints such knee, shoulders, and elbow, for almost 40 decades. Therefore, PMMA is defined as a bioinert and biocompatible polymer with remarkable toxicological safety record, being a Food and Drug Administration (FDA) approved material (Bettencourt & Almeida 2014). For musculoskeletal infections, the use of PMMA as a nanocarrier for the local delivery system may be a more efficient alternative to the conventional antibiotics administration. For this purpose the drug is entrapped or dispersed into a cavity and surrounded by the polymer membrane (Kong 2015).

The major drawbacks associated with this polymer are the fact of being a non-biodegradable and hydrophobic material. The first one may require surgery to remove the material which is painful to patient and high-cost associated. The hydrophobicity affects the drug realising profiles for undefined periods favouring the growth of resistant strains of bacteria (Gomes et al. 2013). Strategies to improve drug release profiles and to avoid drug retention in the reservoir include the synthesis of PMMA composites with hydrophilic polymers.

Eudragit® RL 100 (Eud) is a synthetic polymer, industrially produced and commercialized by Evonik Industries, Germany. Eud is a copolymer of ethyl acrylate, methyl methacrylate and small amounts of methacrylic acid ester (figure 3).

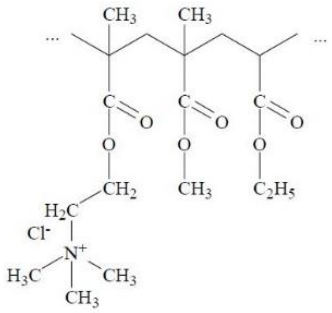

Figure 3: Chemical structure of Eudragit® RL 100. Evonik brochure, accessed on May 12, 2016.

It has in its composition quaternary ammonium groups (positively charged particle) conferring permeability to the polymer (Evonik, accessed on May 12, 2016). Eud is mostly used in pharmaceutical formulations to obtain a controlled and desirable drug delivery performance. It is insoluble at physiologic pH and able to limited swelling, representing a suitable material for drug dispersions (Das et al. 2010). Some studies with PMMA-Eud formulations in antibiotic-loaded microparticles have been already performed showing improved results in permeability, encapsulation, and release profiles when compared with PMMA formulations (Ferreira et al. 2015). Nanoparticles with both formulations were produced with the purpose of exploring new medical features at nanoscale conditions.

1.3.2.1 PMMA and PMMA-Eud Production

Several techniques have been developed for the last decades to produce micro- and nanoparticles. Particles can be prepared from a preformed polymer or by direct polymerization from a monomer solution (Bettencourt & Almeida 2012). The first methodology uses a preformed polymer and it is frequently applied for polymers that cannot be formed by radical polymerization [e.g.,: poly(lactic acid), poly(glycolicacid), etc.]. It comprises salting-out, solvent evaporation, supercritical fluid technology and other processes depending on the main purposes of the study. Direct polymerization, on the other hand, requires a chemical (e.g. ammonium persulphate) or physical initiation (e.g. gamma radiation) and encloses several techniques being emulsion-based procedures the most described in the literature (Ferreira 2015).

PMMA nanospheres have already been characterized and produced by different techniques, but the emulsification-solvent evaporation with a single oil-in-water emulsion (o/w) is still one of the most popular methods. This technology implies an emulsification of PMMA polymer (hydrophobic) in an organic phase using dichloromethane (DCM) as a solvent. Non-ionic surfactants such as poly(vinyl alcohol) (PVA) are also added, providing hydrophilicity to the surface. This composes the aqueous phase of the process (Bettencourt & Almeida 2014). This

step is important to prevent aggregation, a major problem in micro and nanoparticle production. PVA was demonstrated to be an effective surfactant in PMMA formulations. After the emulsification process, the solvent is evaporated by stirring at RT, resulting in precipitation and consequent formation of polymer particles.

In spite of being a fast and easy technique to execute, single-emulsion with solvent evaporation (SESE) has some concerns related to the use of organic solvents and surfactants that may bring some toxicological issues or even deposit in the formulations. Following the International Conference on Harmonization (ICH) guidelines that classify DCM as a Class 2 solvent ("Solvents to be limited"), it restrains the maximal residual concentration to 600 ppm (ICH 2011). Taking this into account, it was demonstrated by Florindo et al. (2010), that is possible to remove great amounts of this solvent after evaporation and keep far behind the established values. All results were confirmed by nuclear magnetic resonance spectroscopy (Bettencourt & Almeida 2012) (Florindo et al. 2010). Furthermore, the washing steps taken by protocol also help to remove some chemical depositions in nanoparticles.

1.4 Characterization of physicochemical properties

The most relevant physicochemical properties that have been shown to affect NP behaviour are presented in figure 4 as their possible impact on cells. Size constitutes the most obvious characteristic to consider. It regulates NP internalization and the ability to trigger or shield our immune system. At the nano level, reductions in size turn into a high surface-to-volume ratio, leading to extremely reactive NPs. Thus, particle size could be directly proportional to its toxicity. For example, smaller particles (<100 nm) tend to cause a higher inflammatory reaction due to their biopersistence in the body (Sutariya & Pathak 2015).

Shape/morphology and surface charge seems to affect NP uptake as well. NPs assume various shapes including fibres, tubes, spheres, etc. This characteristic is deeply connected to membrane wrapping process. Sphere NPs have already shown easier endocytosis when compared to rod or fibre NP (Gatoo et al. 2014). Associated with shape is also toxic. Studies with single- and multi-walled carbon nanotubes present great differences regarding cytotoxic events (Oberdörster 2010). On the other hand, cationic NPs display improved internalization efficacy when compared with anionic or neutral NP, but also induce a higher toxicity when interacting with cellular components (Louro, et al. 2015). Besides, when NPs enter in a biological fluid, a protein coating is formed around the surface. This phenomenon is called "protein corona" and may enhance or reduce the cell uptake (Hocherl et al. 2012). NPs association or dissociation of proteins and current exchange with free proteins present on the boundaries will change some of their physicochemical properties and will mediate the biological response among surfaces and receptors or in the endocytic pathways (Nel et al. 2009). These interactions promote shifts in nanoparticle characteristics, different conformations and depletion of proteins in cellular media.

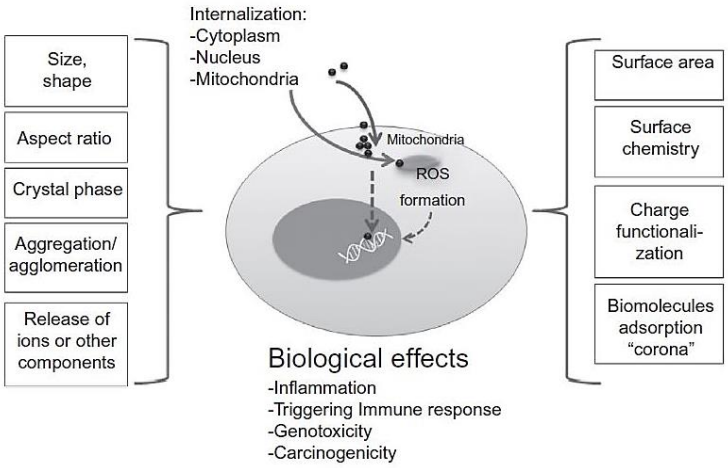

Figure 4: Physicochemical interactions between nanoparticles and biological compartments. Adpated from Louro et al. 2015.

Another important property for analysis is the dynamic behavior of NPs, i.e., aggregates and agglomerates formation. Agglomerates are formed when NPs are dispersed and held together by weak physical interactions leading to the formation of precipitates. This is an easily reversible process. Aggregates instead, are formed by strongly bounded NPs forming a cluster and, for that reason, the process is irreversible (Sokolov et al. 2015). These phenomena are determined by size, surface charge, composition of NPs and the chosen dispersant medium. Accumulation of aggregates for extended periods of time may lead to toxicity and reduced uptake mechanisms for larger particles (Gatoo et al. 2014). Regarding these properties, the size, superficial charge, morphology and aggregation/agglomeration state were evaluated during this work.

Particles size were accessed and measured by laser diffraction, during the NPs production process, in order to correlate how alterations in temperature, medium composition and centrifugal forces can induce size variations. Surface charge was estimated by zeta potential (ζ) after the production process in different dispersant mediums to evaluate how medium compositions interact with the NPs surfaces. Finally, the morphology and consequent agglomerate/aggregate formation was evaluated by Scanning Electron Microscopy (SEM) considering the NPs in their "native state" dispersed in dH_2O and after an incubation with human osteoblast to consider a possible behaviour in an *in vitro* status.

1.5 Cellular interactions and potential toxicity of nanoparticles

1.5.1 Nano-bio interactions

The nano-sized materials and biological structures are within the same size ranges, which facilitate the nano-bio interactions. Indeed, these interactions consist of physicochemical interactions, kinetics and thermodynamic exchanges between the nanomaterial surface and biological entities such as membranes, proteins, organelles and DNA. The differences existent among physical states of a NP and the biological substrates lead also to solid-liquid interactions. When the solid NP is exposed to liquid environments, cells experiment several effects on this interface. The first interactions happen at cellular membrane level where specific (receptor-ligand) and non-specific binding occur. From these interactions, structural, functional and conformational changes may be triggered and developed in biomolecules. Membrane structures are capable of wrap and uptake a NP e.g., by endocytosis, leading to new cellular interactions (inter and intracellular effects) (Nel et al. 2009).

In this perspective, severe effects can be devised from the existing nano-bio interactions at cellular and molecular levels. The importance of understanding and categorizing these outcomes is fundamental to assure the safety of nanomaterials and nanodevices. Recent efforts around the world have been made to recognize the benefits of nanotechnology while minimizing the potential risks. In this context, the “safe-by-design” concept has gained substantial importance over the last years. Reducing population exposure and assuring safe manufacturing processes and reliable products are the gold standard of this approach (Louro et al. 2015). In other words, a material/product should be engineered in its less hazardous nanoform (e.g.size, shape) and in an cost-effective way. Prediction tools such Quantitative Structure Activity Relationships (QSARs), read across and high-throughput screening (*in vitro*/*in vivo*) should be adopted in the early stage to select better formulations (Dekkers et al. 2016). The next step to consider is the exposure risks for the consumers and the environment, and reduce them as possible. Industrial safety procedures include not only secure infrastructures but also safe conditions for workers to handling nanomaterials, storage and transport them. Building a product based on these pillars (safe design, safe use of products and safe industrial procedures) will potentiate a safety course not only in our health but also in the ecosystems (figure 5) (http://www.nanoreg2.eu/safe-design, accessed on Feb. 10, 2017).

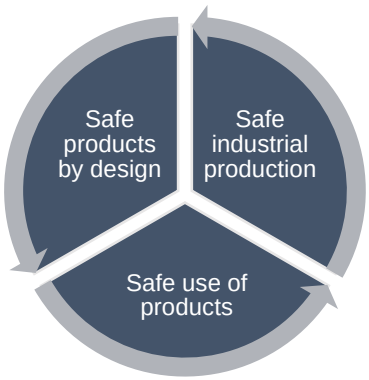

Figure 5: Safe-by-design concept is held by 3 important pillars: Safe design, Safe use of the products and Safe industrial procedures to obtain the final product.

The challenge remains on the fact that nanomaterials with similar chemical composition have quite different behaviors when compared to macroscale materials. In fact, a variation on a specific size, shape, or superficial charge seems to influence its toxicity (Dekkers et al. 2016). Thus, the chemical and physical properties of each nanomaterial should be deeply characterized to better evaluated its potential adverse effects to human health and to the environment.

1.5.2 Nanotoxicology

Furthermore, cell interactions must also be considered within the safety assessment of a nanomaterial. Nanotoxicology is an area of toxicology that addresses the acute and chronic adverse effects of nanomaterials taking into account their psychochemical properties. Nanotoxicology diverges for the conventional toxicology area in that due to their small size, NPs behave differently, resulting in a distinct toxic profile (Bhattacharjee & Brayden 2015).

The mechanisms inherent to NPs toxicity comprise different endpoints and can mediate cytotoxic or genotoxic responses by biological entities. As presented in figure 6, NPs can directly or indirectly induce cellular dysfunctions with impacts on essential cell components: membrane, mitochondria and nuclear compartment. The outcomes from this unbalance, will produce DNA lesions including strand breaks, oxidized and alkylated bases, bulky adducts and intra/inter-strand cross-links (Pillco & Peña 2014). Moreover, genetic instability will modulate inflammatory responses (i.e. macrophages and neutrophils) leading to genotoxicity and cell death (Jiang & Gao 2017). Eventually, chronic inflammation can occur in case of biopersistency and accumulation of NPs in the body. Repair pathways and antioxidant mechanisms work as a first mechanism of cellular defence and DNA repair systems for more depleting effects that cannot be easily repaired.

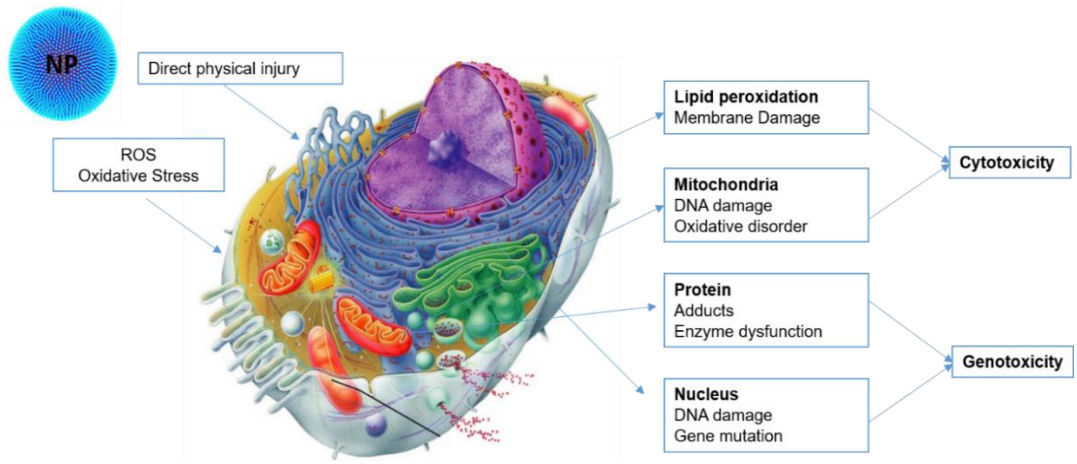

Figure 6: The mechanisms of nanotoxicity under cellular structures. Adapted from (Jiang & Gao 2017), picture available on http://classes.midlandstech.edu/carterp/Courses/bio210/chap03/lecture1.htm.

There are relevant bioassays to assess the toxicity of chemicals and also international recommendations about the most adequate battery of assays that should be used to ensure that a given substance is safe for human health. Considering that NPs are synthesized for biomedical applications, the focus will be on the one hand to understand their biocompatibility and, on the other hand, to assess their potential toxicity. For this purpose, there are still few standard operating procedures to allow the standardization of bioassays towards a complete evaluation of the harmful effects generated by NPs.

1.5.3 *In vitro* experimental models

Cell culture processes are an essential tool for diverse areas and applications. Cancer cells are commonly used since they can be established in simple culture media and proliferate indefinitely, contrarily to non-transformed cells. The most standard systems used for bioassays are adherent two-dimensional (2D) cell monolayer (Edmondson et al. 2014). These cultures represent the gold standard for research although they still provide limited information about the whole-organisms responses (Ravi et al., 2015). In this work, MG-63 a human osteosarcoma-derived cell line from American Type Culture Collection (ATCC ® CRL- 1427 ™) was chosen to assess NPs toxicity. This cell line was derived from an explant culture of a osteosarcoma tissue from a 14-year-old caucasian male. It presents a fibroblast morphology and is adherent under culture conditions. This osteoblastic cell line can be induced to differentiation in culture, thereby allowing to comparatively analyse the toxic effects of nanoparticles in different stages of cell specialization.

1.5.3.1 Osteoblasts

Osteoblasts arise from a mesenchymal stem cell as other different cell types such adipocytes, myocytes, chondrocytes, and fibroblasts (figure 7). Differentiation of osteoblasts is coordinated by several genes, but *Runx2, Sox 9* and *Osterix* are the most important ones. After differentiation, osteoblasts can follow two different paths: they can differentiate into osteocytes embedded in a bone matrix, or in lining cells disposed in the bone surfaces (Grabowski 2015).

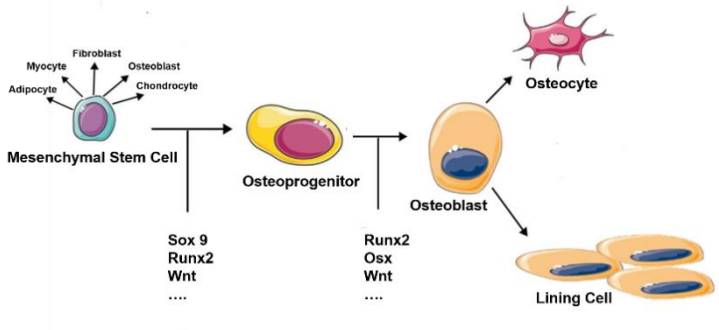

Figure 7: Osteoblast formation and differentiation. Adapted from Arboleya & Castañeda 2013; Grabowski 2015.

Osteoblasts are involved in bone matrix formation and in the regulation of the osteoclasts activity. Osteoblasts have an important role in the organic phase of bone matrix composition (Murugan & Ramakrishna 2005). They secrete collagen (mostly Type I) and non-collagenous proteins. In general, it serves to regulate bone mineral deposition and bone cell activity. The main non-collagenous protein present in bone is alkaline phosphatase. It is a glycosylated protein linked to osteoblast surface, but it can also be found free in mineralised matrix (Clarke 2008, Boskey 2013). This glycoprotein is imperative in bone mineralization, although it is still a poorly understood process (Grabowski 2015). Furthermore, additional glycoproteins are also synthesized by osteoblasts enabling great amounts of calcium and other minerals deposition.

Respecting to osteoblast-osteoclast interaction, it involves important signalling bone mechanisms and the immune system. Osteoblasts trigger osteoclast differentiation via RANK-RANKL (Receptor Activator for Nuclear Factor K Ligand) (Jayakumar & Silvio 2014). Osteoclasts are derived from the macrophage lineage, supporting one of the main functions of this cell line which is bone destruction. Keeping the number and the activity of osteoclasts well controlled is a healthy issue. For instance, if many osteoclasts are active, they will destroy too much bone and osteoporosis will arise, and so, other disorders (Gilbert 2000).

As already referred, osteoblasts are an intrinsic part of bone growth, development, and maintenance. For that reason, the supervision of biochemical and morphological changes of these cells may avoid unhealthy conditions.

1.5.4 Cellular uptake

When a NP is being studied to be used as a nanocarrier, high uptake efficiency must be demonstrated. Different characteristics of NPs can influence the capability of being uptaken by the cell (Singh & Ramarao 2013). Among them, size, chemical composition and the surface charge seem to be those that most influence the NPs internalization. Different mechanisms can be responsible for the cellular uptake of NPs: It can occur by diffusion, by specific transport channels (for smaller particles), or by endocytic pathways. The latter one involve invaginations of the cell membrane (e.g. clathrin or caveolae-mediated systems) or even extensions of cell membrane, including macropinocytosis and phagocytosis (Hocherl et al. 2012). Several studies explore the uptake mechanism without distinguish between the level of internalized and the adsorbed results from NPs. The fluorescence resulting from the interaction between the proteins adsorbed to NPs surface and in the cell membrane provide a global but not a correct signal associated to NPs internalization. This may lead to an unappropriated determination of NPs concentration that actually are internalized. The methodology employed in this work intends to differentiate the intracellular fluorescence by internalized particles from the background fluorescence that comes from the adsorption of nanoparticles on the cell surface. External fluorescence was removed using the vital dye Trypan Blue (TB) that is incapable of penetrating in intact cell membranes and can efficiently quench that background (Vranic et al. 2013).

1.5.5 Cytotoxicity assessment

From a pharmacological point of view, cytotoxicity assays are used as a first screening to test different experimental conditions, observe cellular response and suggest the most appropriated concentration-range to further explore. There are many assays available to characterize the cytotoxic potential of a compound. These assays are usually indicators of cellular damage. Better results are obtained when different endpoints are tested and discussed and thus, complementary assays can be used, depending of the study objective. However, concerns related to NPs adsorption to dyes (e.g. Carbon nanotubes) frequently used to measure cell viability through colorimetric assays may produce false positives and this aspect should be taken into account when choosing a methodology (Bhattacharjee & Brayden 2015). In order to figure out possible cytotoxic outcomes from a PMMA and PMMA-Eud exposure, cell viability and production of reactive oxygen species were monitored.

1.5.6 Oxidative stress

Reactive Oxygen Species (ROS) are chemical species formed upon incomplete reduction of oxygen. It includes O_2^-, H_2O_2 and HO·. These are extremely reactive molecules and interact with different biomolecules such as proteins, phospholipidic bilayer and even with DNA molecules (D'Autréaux & Toledano 2007). For this reason, ROS can induce several adverse effects on cell metabolism, but also can serve as an important intracellular messenger/signalling molecule. In spite of harmful side effects, these molecules are also constantly produced as by-products of aerobic respiration with no damage to cells. To aerobic organisms, it is imperial to assure total detoxification of ROS by cell defence mechanisms in order to maintain a balance between production and removal of oxygen species. When it is not possible to preserve this homoeostasis, oxidative stress is triggered (Held 2012).

Oxidative stress can be quantified in cells in culture based on specific probes, e.g., 2-7' dichlorodihydrofluorescein diacetate (H_2DCFDA). This molecule can pass through cell membranes (figure 8) being hydrolyzed by intracellular esterases. The result is a charged compound that stays trapped inside the cell. If intracellular ROS exists, this enzyme will oxidize H_2DCF to DCF, converting a non-fluorescent compound to a highly fluorescent dye (Chin et al. 2011).

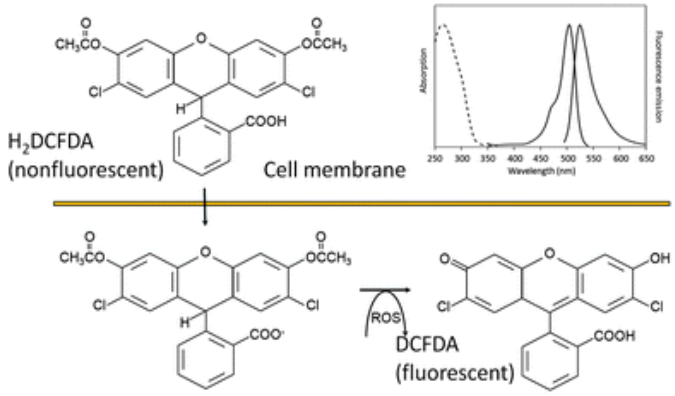

Figure 8: Formation of a fluorescent compound by the specific probe (H_2DCFDA) indicating oxidative stress levels. Adapted from Chin et al. 2011

It is a fast and easy technique that provides information on stress levels from cell populations. This probe is not specific for an individual reactive species, but instead, it seems to react in the presence of any of them, giving a more global response.

1.5.7 Genotoxicity assessment

Genotoxicity assays are presented as a landmark on safety assessment not only for NPs but also for the characterization of other potentially harmful compounds. A NP or a genotoxic agent can interact with DNA or other cellular targets, compromising the integrity of the genetic material. NPs can promote genetic damage either by primary or secondary interactions with DNA molecules. Primary mechanisms can occur by direct or indirect NP-DNA association. Direct primary DNA damage requires NPs internalization into the nuclear compartment provoking physical injury into DNA structure. These will lead to DNA lesions (strand breaks and intercalating NPs with DNA base pairs) or even mutagenic events if it compromises the DNA repair systems. Indirect interactions presuppose that the damage is induced by other molecules (i.e. proteins, repair enzymes, unbalanced ROS production, etc.) that will affect cell replication and division cycles or even the by-products of inflammation that is often triggered by the NPs into the cellular environment. The secondary interactions can be described as the ones that happen between different and organized cells, mostly like it goes on in the *in vivo* situation, during a body stimulus (Evans et al. 2016). It combines different cellular responses and mechanisms that correspond to a more realistic genotoxic evaluation of an NP. This approach can only be explored using *in vivo* models, even though, a plenty of in vitro tests must be performed in a first-line of action to characterize and assess NPs toxicity and to support a safe-by-design practice. Considering the primary interplay of NP-DNA, only a few studies were reported suggesting that NPs can enter in the nucleus and promote direct physical injury to DNA structure. Lovrié et al. (2010) showed that quantum dots within the size range of 2-3nm are able to induce genotoxicity by direct interaction with the main nucleus. Since PMMA and PMMA-Eud are NPs of 500 ± 50 nm size, that pathway will not be considered as a probable mechanism of genotoxic induction. Instead, an indirect genetic damage can be expected to occur.

Alterations at DNA level are intimately connected to several human genetic diseases including cancer. DNA is constantly exposed to mutagenic compounds that can cause serious damage to the human genome. Therefore, the identification of compounds that may have a mutagenic or carcinogenic activity is essential not only for drug development but for controlling human and environmental exposure. Different genotoxicity assays have been developed to detect DNA damage. Procedures that require the use of small cell samples and are able to evaluate DNA damage based on single cell analysis are always valuable.

1.5.7.1 Characterization of the DNA damage: Comet assay

The Single-cell electrophoresis or Comet Assay is a fast and consistent technique to assess DNA damage and repair in individual cells (Glei et al. 2016). For many reasons, the comet assay is an essential tool in toxicological research. It allows to understand background levels of DNA damage in different types of tissues and the ability of cells to respond to a toxic agent and

their repair capacity (Collins 2004). The comet assay *in vivo*, has already been reported in OECD Guideline 489 as a standard test to execute the "Testing of Chemicals" (OECD 2014). It has multiple applications in the detection of genotoxic potential, monitoring tests (ecological/environmental or even human biomonitoring) and in clarifying fundamental mechanisms of DNA damage and repair (Collins 2004). The standard comet assay and a modification using a DNA repair enzyme were used in this work.

The method relies on the migration of lysed cells embedded in agarose on a microscope slide, where an electric current is applied. Agarose assures that DNA is immobilized for the electrophoresis run (Vandghanooni & Eskandani 2011). Alkaline single-cell electrophoresis is performed at a high pH (≈13). This alkaline environment in electrophoresis allows the unwinding of the supercoiled DNA structure. Loops that contain breaks are then extended by electrophoresis process, forming a "comet tail" (Louro, et al. 2015). The alkaline medium also makes comet tails more pronounced and easier to detect (Collins 2004). Using this methodology, it is possible to quantify the level of DNA Strand-Breaks (SB), but it is even possible to increase the assay sensitivity and selectivity by applying lesion-specific enzymes, particularly, glycosylases. These enzymes are able to convert oxidised bases into DNA breaks, increasing the comet tail (Collins et al. 2008). Formamidopyrimidine DNA glycosylase (FPG) is an enzyme capable of detecting adenine and guanine oxidation and convert it into a break (Collins 2004). During this work, the comet assay was executed with and without this modification in order to determine also the level of oxidative lesions comparatively to untreated cultures. Another important aspect to take into account is the comet scoring. Only cells with a clear head and tail should be scored. The percentage of DNA in tail corresponds to the intensity of the comet tail, and it is directly related to the DNA breakage frequency (Glei et al. 2016). The DNA lesions quantified by the comet assay correspond to primary and reversible lesions that can be repaired or, on contrary, lead cell to death if it is highly damaged.

1.5.7.2 Characterization of chromosome damage: Cytokinesis-Block Micronucleus Assay

Severe DNA damage may be not reversible by cellular mechanisms of repair thereby resulting in permanent damage to the cell. On the other hand, the cell cycle can be blocked in an attempt to allow DNA repair and, if this is not possible, the programmed cell death (apoptosis) can be triggered. Another possibility is the progress of cell division where the DNA damage is transmitted to daughter cells either as gene mutations or as chromosome aberrations, inducing deleterious defects and leading to cell transformation (e.g. carcinogenesis). The *in vitro* Cytokinesis-Block Micronucleus Assay (CBMN) is an efficient methodology, with international

validation and described in OECD Guideline 487 as standard procedure for detect genotoxic events at the chromosome level.

The Micronucleus assay is one of the most important *in vitro* procedures to assess genetic damage and characterize cytotoxicity and genotoxicity of a specific compound/chemical (Fenech 2000). When cells experience high levels of toxicity, micronucleus (MNi) can reflect a pronounced effect of chromosome damage (loss or breakage). They originate from chromosome fragments (acentric fragments) and/or whole chromosomes that are incapable of migrating to the poles of the cell at anaphase stage (Fenech et al. 2003). A nuclear membrane is formed around the genetic material and this corpuscle remains in the cytoplasm, morphologically similar to main nuclei but smaller, which gave origin to the term “micronucleus” (Fenech 2000). MNi could be only expressed in “active cells” that are able to complete cell cycle, so it is important to restrict and distinguish cell population between dividing and non-diving cells. The CBMN assay is a slight modification form of the traditional methodology since it allows this selection by addition of cytochalasin-B (Cyt-B). Cyt-B is an inhibitor of actin polymerisation, essential to individualize the two daughter cells in cytokinesis phase and thus its effect results in a binucleated cell following the mitosis (Fenech 2007).

CBMN is also used to measure other important endpoints related to chromosomal abnormalities such as: nucleoplasmatic bridges (NPBs); nuclear buds (NBs); cell viability (necrotic and apoptotic aspect) (figure 9) and cytostatic effects.

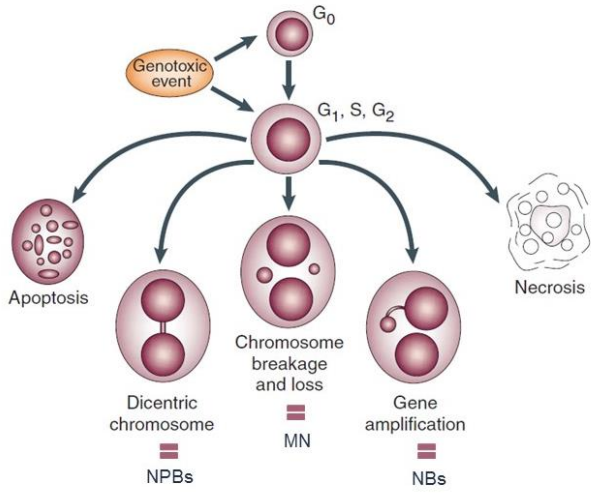

Figure 9: The various possible fates of cultured cytokinesis-blocked cells following exposure to cytotoxic/genotoxic agents. Adapted from Fenech, 2007.

The NPBs are formed from dicentric chromosomes that are pulled to opposite poles of the cell in anaphase, the NBs and MNi have homologous structure, but NBs are still linked to the main nucleus and is an important biomarker for gene amplification. Cytostasis represents the ratio between mononucleated, binucleated and multinucleated cells in a population. All of these parameters improve the detection of possible toxicological effects induced by a chemical compound or nanomaterial.

2. Objective

This projected was aimed at assessing the safety of polymeric nanoparticles developed as nanocarriers for drug delivery, in a human osteoblast cell line. To achieve this purpose, the following specific objectives were defined:

1) Production of plain PMMA and PMMA-Eud (50:50) with an average distribution size range of 500 nm.

2) Physicochemical characterization of both sets of nanoparticles considering the different conditions experienced not only in particles production and storage but also in cellular studies.

3) Biosafety evaluation through cytotoxicity and genotoxicity characterization in a human osteoblast cell line.

3. Methodology

3.1 Nanoparticles Production

3.1.1. Single Emulsion Solvent Evaporation (SESE) method

Polymers were weighted for both formulations (Table 1) in small glass bottles (PMMA- Sigma Aldrich (UK); Eud was kindly provided by Evonik Degussa International AG (ES)). Then were diluted in defined values for DCM for a few minutes until a homogenous solution was obtained (figure 10: initial stage). In a beaker, 30 mL of PVA 5% (poly(vinyl alcohol), (87%-89% hydrolysed v/v) (Sigma-Aldrich UK) (diluted in dH_2O) were added to the solution and mixed by Silverson mixer emulsifier (L5M, Silverson, UK) during ten minutes at high shear velocity (figure 10: NPs formation). This step is essential to obtain the single emulsion (w/o mixture) and the consequent NPs formation. After this stage, samples remained in a fume hood by magnetic stirring conditions (350 rpm) (Multipoint 15, Varomag, UK) for four hours. Succeeding this, 1 mL of D(+)-Sucrose (10%, w/V) (Applichem, Germany) was added to each batch and immediately centrifuged (64R, Allegra™ Beckman Coulter, USA) at defined conditions. After that, the supernatant was discarded and add 1 mL of D(+)-Saccharose(10%, w/V) (diluted in dH_2O) and 20 mL of sterile/filtered water. A second centrifugation was executed, and each formulation was kept in 5 mL of D(+)-Sucrose (0.5%, w/V) at -4°C.

Table 1: Conditions applied for each formulation.

Batch Composition	PMMA (mg)	Eud (mg)	Total mass (mg)	DCM (mL)	5% PVA (mL)	Centrifugation (Time, 4º C, rpm)
PMMA	65	-	65	7.5	30	(20, 17500) × 2
PMMA-Eud	62.5	62.5	125	5	30	(10, 7500) × 2

Lyophilisation is a widely used technique in pharmaceutical industries to increase shelf life and chemical stability of products. In this work, NPs were lyophilized using a Freeze-Dryer (Alpha 1-4 (100-400), Christ, Germany). After lyophilisation (figure 10: final stage), particles can be easily reconstituted, and dry powders formulation can reduce contaminations since the whole particle production was not performed in sterile conditions.

This process allowed the calculation of the yield of production obtained in each batch, following the next formula:

$$\eta\,(\%) = \frac{\boldsymbol{Pratical\ mass\ obtained}}{\boldsymbol{Theoretical\ mass}} \times \mathbf{100} \qquad \text{(Equation 1)}$$

Loaded particles with Coumarin 6 (98%, Sigma-Aldrich, UK) followed the same production steps, except for dilution in DCM, where it was added 70 µL of the respective dye (10mg/mL). These particles were used to perform the uptake assay.

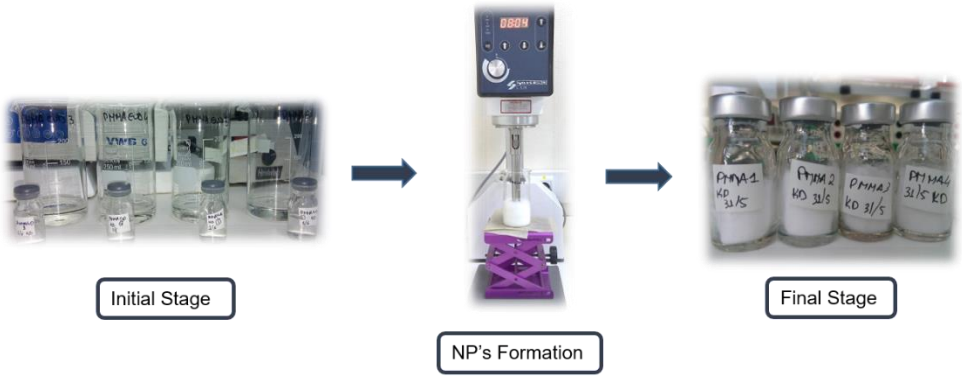

Figure 10: NPs production process involves different steps to obtain the final product.

3.2 Physicochemical Characterization

3.2.1 Particle Size Analysis

Measurements were carried out by Laser diffraction technique using a Mastersizer 2000 - Hydro 2000S (Malvern Instruments, UK) based on ISO 13320 (2009), which is applicable to particle sizes ranging from 0.1 µm to 3 mm (http://www.iso.org/iso/catalogue_detail.htm?csnumber=44929). This method is based on Mie's theory. It was developed to predict the way of light is scattered by spherical particles and how the light is absorbed, or passes through the particle. Measurements consider a scattering pattern that is formed by a field of particles.

The amount of sample required for each size determination was related to reach 5% of "Obscuration". This specific criterion indicates the ideal amount of sample to assure good and reproducible results. The output data given by software, display the size values by percentiles: d(0.1); d(0.5) and d(0.9) where for e.g. d(0.1) represents the size (µm) of particle below 10% of the whole population. In this work, only d(0.5) was analysed. Span is another important element to consider. Span is a measurement of distribution range and for that reason should not be larger than 1. It can be calculated by (Malvern Instruments Ltd 2007):

$$\boldsymbol{Span} = \frac{\boldsymbol{d}(\mathbf{0.9}) - \boldsymbol{d}(\mathbf{0.1})}{\boldsymbol{d}(\mathbf{0.5})} \qquad \text{(Equation 2)}$$

During the NPs production, size distribution was assessed (volume-based), after solvent evaporation, after both centrifugations (supernatant and pellet homogenised), after freezing and lyophilisation. NPs suspensions were carefully homogenised using purified water as a dispersant and added to a specific reservoir on the equipment. Particle size determination was executed under constant agitation (1750 rpm), in room temperature (RT), and for PMMA-Eud was also applied 80% of ultrasounds in frozen samples. NPs were also submitted to incubation with complete medium RT and at 37 °C, trying to mimic in vitro conditions in cellular assays.

Three batches of each nanoparticle formulation were analysed (n=3) and five measurements were performed for individual samples. Values were analysed using a One-way ANOVA and Post-hoc Tukey's multiple comparison test (GraphPad PRISM 5 software, USA).

3.2.2 Surface charge

Particles surface charge was measured by zeta potential considering the electrophoretic mobility. An electrical field is applied across the sample and the movement/velocity of the NPs (electrophoretic mobility) can be determined by Laser Doppler Velocimetry (LDV) (Walker, 2011).

Once the NPs are introduced in the electrophoretic cell, they move towards the electrode of opposite charge, and their velocity is measured and expressed in unit field strength as their mobility (figure 11). These calculations are based on Henry's equation that relates how electrophoretic mobility depends on the zeta potential of the particle itself, on the dielectric constant and the viscosity of the dispersant medium (Malvern instruments 2004).

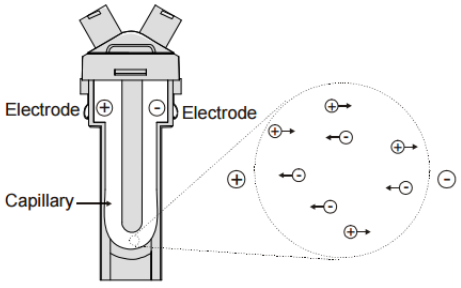

Figure 11: Standard Electrophoretic cell, containing two gold electrodes (with opposite charges). Adapted from (user manual).

Samples (PMMA and PMMA-Eud) were injected in electrophoretic cell, with a syringe and diluted in 3 mL of filtered dH_2O. Those cell was introduced in Malvern Zetasizer Nano Z (Zen 2600, Malvern Instruments, UK). Measurements were carried out at 25°C, in dH_2O and complete

medium for both formulations. For each sample, three individual measurements were executed and one batch for each nanoparticle.

3.2.3 Scanning Electron Microscopy (SEM) Analysis

SEM is a form of electron microscopy and a well-accepted technique to characterize nanoparticles dispersions or to explore biological systems. It scans a sample using a focused electron beam of high-energy and produces images with information about topography and composition. SEM is composed by an electron source, electromagnetic lenses and an electron detector. The electron beam is accelerated and focused. When it reaches the sample, the energy of the electron beam is dissipated in many signals, but the most important are the secondary electrons generated in the ionization process. These secondary electrons emitted by the sample are then detected, producing specific signals and patterns revealing information on external morphology, structure and chemical composition (Egerton 2005). SEM can provide a magnification of objects of 10 nm and, for that reason, precise measurements of small structures (< 50 nm) are also a powerful feature of this technique as well as critical for nanomaterials physicochemical characterization (Knott & Genoud 2013).

SEM analysis were obtained from NPs dispersions and undifferentiated osteoblasts were exposed to both NPs formulation. Lyophilised NPs were reconstituted in dH_2O (to a final concentration of 20 mg/mL), air-dried and analysed. For the cell incubation, undifferentiated MG-63 cells were rinsed with Trypsin-EDTA for 4 minutes at 37ºC. Complete medium was added to inactivate detachment. Cells were then plated at density of $1x10^4$ cells/mL in 15mL tubes. NPs solution were added at final concentration of 0.5 mg/mL and incubated for 3 hours at 37ºC, 5% CO_2. When time was reached, suspensions were centrifuged at 1200 rpm, 5 minutes. Medium was removed and 800 µL of DPBS were added to each tube. Pellet was gently homogenised. This process was repeated twice.

Dispersions were attached in a double sided carbon adhesive over the sample holder (figure 12). Preparations were air-dried for 30 minutes and then analysed recurring to a Hitachi TM3030 Plus microscopy.

Figure 12: Sample holder containing double sided carbon adhesive. Samples were divided following the numbers: 1- PMMA; 2- PMMA incubated with cells; 3- PMMA-Eud; 4- PMMA-Eud incubated with cells.

3.3 Cellular Assays

3.3.1 Cell Maintenance

Undifferentiated MG-63 cells (ATCC® CRL-1427™) were maintained in complete medium composed by RPMI 1640 (1X) (Gibco, Scotland, UK) supplemented with 10% heat-inactivated Fetal Bovine Serum (FBSi) (Thermo Scientific, Waltham, USA) Penicillin/Streptomycin mix (Pen/Strep; with 10000 units/mL of penicillin and 10000 µg/mL of streptomycin, Gibco, Scotland, UK) 2mM L-glutamine (Life Technologies, UK). Cultures were maintained in an incubator at 37ºC, 5% CO_2 until sub-confluence (approximately 80%) was reached. Subcultures were obtained by cell detachement with trypsin-EDTA (0.05%) (Gibco, Scotland, UK) incubated for 4 minutes at 37ºC, followed by inactivation with complete medium and appropriate dilution.

After this procedure, cell viability was accessed using the dye exclusion assay with Trypan Blue. Trypan Blue (0.4%) (Gibco, Scotland, UK) is a vital stain that allows distinguishing viable and non-viable cells. This compound can only permeate disrupted membranes, colouring dead cells in blue. Using a Newbauer's chamber, cell counts were carried out and cell viability and density were then estimated. Usually, cells with $3x10^4$ cells/mL density were transferred to new culture flasks until sub-confluence was achieved.

3.3.2 Differentiation assays

To induce cell differentiation, complete medium was supplemented with the following osteogenic additives: 10mM β-glycerophosphate (Sigma, USA), 50 µg/mL ascorbic acid (Sigma, USA) and 10nM dexamethasone (Sigma, USA). MG-63 cells were cultured under differentiation medium conditions for 72 hours, at 37ºC, 5% CO_2. When, subconfluence was achieved, alkaline phosphatase (AP) and Calcium deposition assays were conducted.

3.3.2.1 Alkaline phosphatase activity

In a 96-well plate, differentiated MG-63 cells, undifferentiated MG-63 and HEK293T cells(ATCC®CRL-3216™) were seeded at a final density of $0.5x10^5$ cells/mL and incubated for 24 hours at 37ºC, 5% CO_2. When the time was reached, cells were lysed with 0.02% SDS solution and incubated with p-nitrophenyl phosphate in an alkaline buffer solution (pH=10.3) (N7653, Sigma Aldrich, USA) for 30 minutes, 37ºC. The hydrolysis of the p-nitrophenyl phosphate allowed to determine the presence of AP in cell lysates. The reaction was stopped with NaOH (1M) (Merck). Absorbance values were assessed during three hours' minute by minute, at 405 nm. The Bicinchoninic Acid Assay (BCA) method was also performed in order to quantify the amount of total protein on the lysates. Successive dilutions concentrations (2 mg/mL; 1mg/mL; 0.5 mg/mL; 0.250 mg/mL; 0.125 mg/mL; 0.06 mg/mL; 0.03 mg/mL; 0 mg/mL) were added and served as a standard for protein quantification. The defined concentrations of Bovine Serum Albumin (BSA) protein allows to determine a calibration curve and to estimate the total protein present in the AP assay. Data from 8 replicates will be presented considering mg of total protein/mL.

3.3.2.2 Calcium deposition

Calcium deposition was assessed by alizarin red staining (Sigma-Aldrich, St Louis, MO). In a 96-well plate, differentiated MG-63 cells, undifferentiated MG-63 and HEK293T were seeded at a final density of $0.5x10^5$ cells/mL and incubated for 24 hours at 37ºC, 5% CO_2. Then, alizarin red was added to 0.1% NH_4OH (pH= 4.2) solution and incubate for 20 minutes at RT. To quantify the stained calcified deposits, wells were washed four times with MiliQH_2O, while shaking for 5 minutes. The precipitate formed was solubilized with 5% SDS in 0.5M HCl (Applichem, Germany) for 30 min at RT. The well content was transferred to another 96-well plate, and absorbance was measured at 405 nm. The BCA test was also executed in the same conditions described above. To each cell type, 8 replicates were considering regarding the mg of total protein/mL.

3.3.3 NPs Solution

Lyophilized NPs were dispersed using bidestilated sterile water (injectable quality) to a final concentration of 20 mg/mL. For cells exposure, nanoparticle suspensions were then diluted in complete culture medium without any osteogenic compounds. These solutions were always freshly prepared and applied immediately to prevent particles deposition or small aggregates. The concentrations range was chosen based on some guidelines (OECD 487) and previous work performed by Graça (2014). Table 2, presents the NPs concentration (mg//mL and $\mu g/cm^2$) used in the different cell assays.

Table 2: NPs concentration used on cellular assays in different well-plates.

Concentration (mg/mL)	Concentration (µg/cm^2)		
	MTT (96-well plate)	**Comet Assay (24-well plate)**	**Micronucleus assay (6-well plate)**
0.05	5.56	13.89	15.79
0.1	11.11	27.78	31.58
0.5	55.56	138.89	157.90
1	111.11	277.78	315.79
2	222.22	555.56	631.58
5	555.56	1388.89	1578.94

3.3.4 Uptake Assay

MG-63 cells were grown in differentiation medium for 72 h, 37ºC, 5%CO_2. After that, cells were seeded in a 96 well plate at a density of 1x10^5 cells/mL and incubated for 24 h, in the same conditions. Later on, the culture medium was removed and replaced by 0.05 mg/mL and 0.1 mg/mL of Coumarin 6 (98%, Sigma Aldrich, UK) loaded NPs. Fluorescence was measured (Excitation wavelength: 485 nm; Emission wavelength: 520nm) and the obtained values were defined as "Background fluorescence". After that, cells were incubated with those NPs for 1 h, 37ºC, 5% CO_2 and the fluorescence was immediately measured and defined as "Absolute Fluorescence". 50µL of Trypan Blue [0.4% (v/v)] was added to each well and fluorescence was measured again. The values acquired are the real measurements of particles internalization. In order to normalize the results obtained, a BCA assay was performed as previously described in the AP assay. Complete medium and Trypan blue was removed and cells were washed thrice with PBS (1X, Gibco, Scotland, UK). This is another important step since Trypan blue has shown to induce some toxicity in cells when incubated for short periods of time and the great amount of proteins in FBS could have interfered with the total protein measurements. After the washing steps, 50 µL of NaOH (0.1 N diluted in PBS) was added and left incubated for 30 minutes, 37ºC, 5% CO_2. Successive dilutions of BSA protein (2 mg/mL; 1mg/mL; 0.5 mg/mL; 0.250 mg/mL; 0.125 mg/mL; 0.06 mg/mL; 0.03 mg/mL; 0 mg/mL) were added and served as a standard for protein quantification. During 30 min, the plate was incubated at 60ºC, 5% CO_2 and fluorescence was instantly measured (Excitation: 420 nm Emission: 565 nm). The concentrations defined for BSA allows to determine a calibration curve and to estimate the total protein present in the uptake assay. The results may be presented as mg of total protein.

A preliminary test had been executed to determine the concentration of Trypan blue needed to achieve the total fluorescence quenching of the fluorochrome Coumarin-6. This test consisted of measuring the fluorescence of a 96 well-plate loaded with NPs only and its decrease following addition of Trypan blue until the fluorescence disappears. This is an important step since it is essential to quantify the cell uptake of both particles.

Data from 10 replicates were presented as mg of total protein for each tested concentration and NP. As negative control was considered differentiated MG-63 only with complete medium, that was also quenched with TB and this data was used as the background of untreated cells. One-way ANOVA and Post-hoc Tukey's multiple comparison test was used to analyse the uptake data (GraphPad PRISM 5 software, USA).

3.3.4.1 Fluorescence Microscopy

In order to assure more reliability of the uptake assay, cells were observed under fluorescence microscopy. Different staining procedures were conducted to identify cellular structures and the same Coumarin-6 loaded particles were used. For cytoplasmic compartment labelling, the Rhodamine-phalloidin probe was used and that is highly selective to label F-actin. This protein can be easily found in the cytoskeleton of eukaryotes and for that reason defines the cell boundaries. Furthermore, DAPI (4',6-Diamidino-2-Phenylindole, Dihydrochloride) was also used to stain the nuclear compartment of cells. It is a nucleic acid stain (especially for adenine - tyrosine clusters). With this multicolour fluorescence technique, it is possible to define approximately NPs location inside the cells.

This procedure was conducted in conditions similarly to those used in the previous cell uptake assay. The same cell density, culture medium, NPs concentrations and time of incubation were maintained. Differentiated MG63 cells were grown on 24-well plates containing sterile glass coverslips (Greiner, Germany) during 24 hours at 37ºC, 5% CO_2. When time of NPs exposure was reached, cells were rinsed thrice with 5 mL PBS (10mM) containing glycine (20mM) at pH 7.4. The cells were fixed with 4% (w/v) paraformaldehyde (Sigma-Aldrich, UK), protected from light and at RT and were washed again thrice with PBS + Glycine solution as previously described. Cells were then permeabilized with 0.5% Triton X100 for 4 minutes and rinsed three times with PBS+Glycine solution. Cells labelling was performed with 1 mL of Rhodamine-phalloidin (6.6 µM) (Life Technologies, UK) and staining with DAPI (Life Technologies, UK) diluted in PBS (10 mM) during 45 minutes at RT (protected from light). After that, cells were rinsed three times with PBS + Glycine solution. The coverslips were air dried and mounted using fluorescent mounting medium ProLong® Gold antifade reagent (Life Technologies, UK).

Fluorescence was observed and recorded on Axioscop 40 fluorescence microscope (Carl Zeiss, Germany) equipped with an Axiocam HRc (Carl Zeiss, Germany) camera. Image acquisition was possible using the software AxioVision Rel. 4.8.1 (Carl Zeiss, Germany). The merged images were obtained using the Image J v.10 software.

3.3.5 Cytotoxic Assays

3.3.5.1 Viability Assay

To assess cell viability, the MTT [3-(4,5-dimethylthiazol-2-yl)-2,5-diphenyltetrazolium bromide] assay was used in the present work. It is based on the reduction of yellow tetrazolium into formazan crystals by viable cells (figure 13) (Walker, 2011). This assay relies on the mitochondrial activity of cells, where the action of specific enzymes (dehydrogenases) produce reducing molecules such NADH that transfers electrons to MTT (Sittampalam et al. 2016). The resulting product has a characteristic absorbance value and can be measured by spectrophotometric methods. Contrarily, non-viable cells are unable to reduce MTT. Therefore, formation of intracellular formazan is directly proportional to the number of viable cells (American Type Culture Collection 2011)

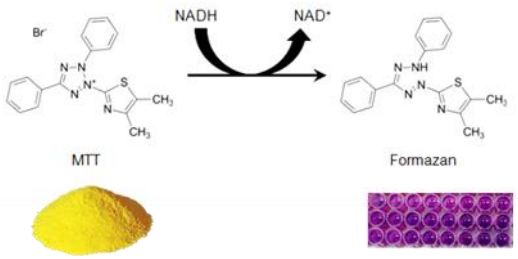

Figure 13: Structure of MTT and the coloured formazan product. Adapted by Sittampalam et al., 2016

Undifferentiated MG63 cells were plated at a density of $1x10^5$ cells/mL in a 96 well plate, for 24 hours, 37º C, 5% CO_2. When time was reached, cells were exposed to PMMA and PMMA-Eud treatment during 24 and 64 hours at 37ºC, 5% CO_2. For positive control, SDS [0.07% (v/v)] was chosen and added 1 h before incubation time ended. After that, medium was removed and cells were washed twice with 100 µL of PBS. MTT solution (0.5 mg/mL) was added and plates incubated for 3 hours in previously defined conditions. The solution was removed and 100 µL of DMSO were added to each well. Plates were kept for 30 minutes under agitation and light protected. Then, absorbance was measured at 570 nm in a Multiskan Ascent Spectrophotometer (Thermo LabSystems, Waltham, MA) and using a reference filter of 690 nm.

A previous test was executed in order to define an appropriated cell density and an effective concentration of SDS. A calibration curve was traced and 0.07% (v/v) SDS value was achieved (data not shown).

An interference test between the MTT and NPs was also performed for all defined concentrations tested to understand if there is any interactions that could lead to false positives or background interference of the NPs. PMMA and PMMA-Eud were plated with MTT (0.5 mg/mL) and incubated for 3 hours. After that, medium was removed and DMSO was added and kept for 30 minutes under agitation and light protected. When time was reached, fluorescence was immediately read using the same equipment.

For both NPs formulation, 3 independent assays were carried out, and 6 absorbance values were considered for each condition. Absorbance values were converted to cell viability (%) as the following equation:

$$\boldsymbol{Cell\ Viability}\ (\%) = \frac{\bar{x}\ \boldsymbol{Absorbance}_{(\lambda=570\ nm)}\ \boldsymbol{for\ Treated\ Cultures}}{\bar{x}\ \boldsymbol{Absorbance}_{(\lambda=570\ nm)}\ \boldsymbol{for\ Untreated\ Culture}} \times \mathbf{100} \qquad \text{(Equation 3)}$$

Statistical analysis was performed by One-way ANOVA analysis, with Post-Hoc Tukey test (IBM SPSS Statistics v.20.).

3.3.6 Reactive Oxygen Species (ROS) production

Oxidative stress response was accessed in differentiated MG-63 cells using H_2DCFDA. Cells were plated in 96 well plate at density of 1×10^5 cells/mL and incubated for 24 hours at 37°C, 5%CO_2. After that, medium was removed and replaced by fresh medium without osteogenic additives, since ascorbic acid is a well-known antioxidant and interferes with oxidative stress results. Cells were incubated with the fluorescent dye for 30 minutes at 37ºC, 5% CO_2. At the same time, H_2O_2 was also added to the respective wells and served as a positive control of the assay. The medium was then removed and replaced by fresh medium. MG-63 cells were then exposed to the previously defined concentrations of PMMA and PMMA-Eud during 1 and 3 hours, at 37ºC, 5% CO2. When the incubation time was reached, the fluorescence was immediately measured in a microplate reader (FLUOstar BMG Labtech, Germany) (Excitation: 485 nm, Emission: 520 nm). For each condition tested, 12 replicates were analysed for both NPs.

Data may be presented as a Relative Fluorescence Units (RFU) in percentage (%) and can be calculated based on the fluorescence ratio:

$$Fluorescence\ Ratio\ (RFU\ \%) = \frac{Fluorescence\ of\ Treated\ Cells}{Fluorescence\ of\ Untreated\ Cells} \times 100 \qquad \text{(Equation 4)}$$

For statistical analysis, One-way ANOVA with Post-Hoc Tukey's multiple comparison test was used (GraphPad PRISM 5 software, USA).

3.3.7 Genotoxicity Assays

3.3.7.1 Comet Assay

Undifferentiated osteoblasts were cultured in a 24-well dish at a density of $1x10^5$ cells/mL and incubated for 24 h, at 37ºC, 5% CO_2. After 24 h, cells were exposed to PMMA or PMMA-Eud concentrations as described in "Nanomaterial Preparation". For each NP, two time-points were tested: 3 h and 24 h. Incubations took place at 37ºC, 5% CO_2. To induce DNA damage, Ethyl Methanesulfonate (EMS) was selected as the positive control (1h exposure). EMS was previously diluted in PBS and then in complete culture medium to a final concentration of 5mM. When time was reached, cells were washed with PBS and detached using Trypsin-EDTA as described above. Cell suspensions were transferred to 1,5 mL tubes and centrifuged for 5 min, 1200 rpm, 4ºC. Supernatant was discarded and the pellet was gently resuspended. A previously warmed (37ºC) 0.8% low melting point agarose were added to each tube, homogenised and placed on a pre-coated (1% agarose) microscope slide. Coverslips were immediately added to each drop and placed on a cold box to assure agarose solidification. After 10 min, coverslips were removed and slides transferred to a copplin jar, protected from light and with fresh cold lysis solution [89% (NaCl (2.5 M); $Na_2EDTA.2H_2O$ (100 mM); Tris-HCl (10 mM); NaOH (10 M)); 1% Triton X; 10% DMSO]. Incubation proceeded for 2 h, at 4ºC. Slides were then washed with F buffer [HEPES (40 mM); KCl (0.1 M); EDTA (0.5 mM); BSA (0.2 mg/mL); pH= 8] thrice, 5 min each. The FPG enzyme (gently provided by A. Collins, Oslo University, Norway) was unfrozen and diluted in F buffer. To each gel formed over the slide, FGP enzyme or F buffer solution were applied and a coverslip placed on the top. The incubation took place in a humidified chamber for 30 min, at 37ºC. Coverslips were removed and slides placed in an electrophoretic cell surrounded by ice. Slides were covered with electrophoresis buffer [NaOH (300 mM); $Na_2EDTA.2H_2O$ (1 mM); pH= 13] during 30 minutes. After DNA denaturation, amperage and voltage were defined at 300 mA and 28 V, respectively. Electrophoresis was executed during 25 min, at 4ºC. When time was reached, slides were washed with cold neutralization buffer [Trizma Base (0.4 M); HCl (0.4 M); pH= 7.5] for 10 min. followed by cold MilliQ/dH_2O for 10 min. Slides were then transferred to a box a protected from light and air dried until analysis

Microgel staining was performed with Ethidium Bromide (12.5 µg/mL). Slides were covered with coverslips and placed in a humid box protected from light and let incubate for 30 min, 4ºC. All measurements were conducted under a fluorescence microscope (Axioplan2 Imaging, Zeiss) using the Comet Imager 2.2, MetaSystems Software.

Two independent assays were performed and in each assay two replicates were made for each condition tested. From each well, 2 gels were done and 50 cells were counted per gel, 100 cells per culture, 200 cells per treatment (figure 14). For FGP treatment, same analysis was performed in individual slides.

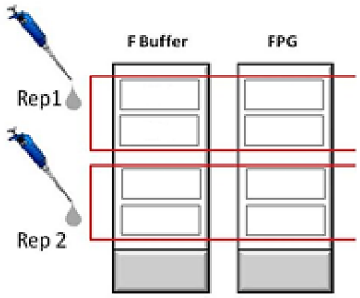

Figure 14: Sample distribution on slides for comet assay in FPG and Non FPG treatments.

Data are expressed as the % DNA in tail (Mean ± SD). Statistical analysis was carried out considering that data followed a normal distribution (IBM SPSS Statistics v.20.). One-way ANOVA test and Tukey's Post-Hoc test was used to evaluate data. Differences between the conditions with and without FPG were analysed using Student's t-test.

3.3.7.2 Cytokinesis-Block Micronucleus Assay (CBMN)

MG-63 cells were seeded in 6-well plates at a density of $1x10^5$ cells/mL for 24 hours, at 37°C, 5% CO_2. Then, medium was removed; treatment was applied in the previously defined concentrations and incubated for more 22 hours in same conditions. At 22 hours of exposure, Cyt-B (final concentration 4 µg/mL) was added to all wells and cells were incubated for more 42 h in same conditions (total time of exposure to NPs= 64h). Mitomycin C (MMC) was chosen as the positive control since it produces chromosome breaks and is generally used as a genotoxic agent for tumour cells (OECD Guidline 487, 2010) (Rassoolzadeh et al. 2016). MMC was added to 45h cultures at a final concentration of 0.10 µg/mL (diluted in PBS and culture medium) and incubated for 1 hour before Cyt-B addition.

Following this step, the medium was removed, cells were washed twice with PBS, detached with trypsin-EDTA and inactivated with fresh medium. They were centrifuged for 5 min at 1000 rpm, the supernatant was discarded and the pellet was re-suspended. Cells were submitted to a hypotonic treatment by addition of 5mL of previously warmed KCl (0.1M) solution to each 15ml tube, drop-by-drop, while vortexing. These tubes were immediately centrifuged at 1200rpm during 5minutes. The supernatant was discarded and the pellet was re-suspended. The cells were fixed using a previously cold fix solution (3:1 MetOH:COOH) drop-by-drop, while vortexing. The spread was made using a cytocentrifuge (1000 rpm, 5 min), and cell density was verified and adjusted for each slide. All slides were air-dried for 24 h. The staining was executed with a 4% Giemsa solution (Giemsa stock solution was filtered with a Millipore paper and diluted in Gurr's phosphate buffer). Slides were mounted with 2 drops of Entellan and a coverslip.

A preliminary assay was conducted in order to optimize several conditions which are specific for this cell line and these NPs. The cell density, MMC and Cyt-B concentration over time of incubation, the hypotonic treatment and the spread were all adjusted.

The criteria for cell selection and scoring in CBMN assay, has been described and well-characterized by Fenech (2000), and for that reason it will not be exhaustively described in this work. Nevertheless, there are some important issues to refer: in each condition should be analysed 2000 cells (2 independent cultures per condition, 1000 cells per culture); two different scores need to be made, 500 cells for percentage of mononucleated, binucleated and multinucleated cells and another 500 cells for MNi, NB's and NPBs frequency, completing the 1000 cells required. Cells should have a well-limited cytoplasm and normal nucleus morphology. MNi should only be considered if had until 1/3rd diameter of the main nuclei. NBs have to be linked to main nucleus and NPBs have to have a width of 1/4th of the diameter of the nuclei. All of these biomarkers should have the same staining intensity as the main nuclei.

Based on mono, bi and multinucleated index, it is possible to quantify the cell proliferation capacity or cytotoxic effects caused by the tested compound. The Cytokinesis-Block Proliferation index (CBPI) and Replication Index (RI) were calculated as presented below in equations 5 and 6 (OECD Guidline 487, 2010):

$$\boldsymbol{CBPI} = \frac{(\boldsymbol{Mononucleate\ cells})+(2*\boldsymbol{Binucleate\ cells})+(3*\boldsymbol{Multinucleate\ cells})}{\boldsymbol{Total\ number\ of\ cells}} \qquad \text{(Equation 5)}$$

$$\boldsymbol{RI} = \frac{\left(\frac{(\boldsymbol{Binucleate\ cells})+(2*\boldsymbol{Multinucleate\ cells})}{\boldsymbol{Total\ number\ cells}}\right)\boldsymbol{Treated}}{\left(\frac{(\boldsymbol{Binucleate\ cells})+(2*\boldsymbol{Multinucleate\ cells})\ \boldsymbol{Control\ cells}}{\boldsymbol{Total\ number\ of\ cells}}\right)\boldsymbol{Untreated}} \times \mathbf{100}\% \qquad \text{(Equation 6)}$$

Using a *blind-scoring* for optic microscopic analysis (Axioskop 2 Plus, Zeiss), MNi, NBs and NPBs were analysed at 100x magnification. For mono, bi and multinucleated scoring 40 xs magnification was used. Apoptotic and necrotic cells were not considered in this work. The statistical analysis of CBPI and RI was performed using Student's t-test for comparison of paired samples. For MNi, NBs and NPBs assessment, two-sided Fisher's exact test was used (IBM SPSS Statistics v.20.).

4. Results

4.1 Nanoparticles Production

As previously described, both sets of NPs were produced by the SESE technique. Following the purification processes, samples were lyophilized and kept in a sealed glass vial to maintain the NPs properties more stable for extended periods of time. Besides, it allows long-term storage at RT as long as the vials remain intact. The same procedure was used for Coumarin-6 loaded NPs.

The yield of production, accessed with basis on the final mass obtained after lyophilization for each batch (6 batches from each nanoparticle) are presented in Table 3. It is evident the disparity existent between the values obtained for each NP formulation. The first formulation, PMMA NPs, presents a quite satisfactory result since the yield almost reaches the 100%. However, when Eud is added to the formulation in equal parts (50% PMMA; 50% Eud) the yield of production highly decreases. Only 30% (approximately) of the polymers are recovered, reflecting a reduction of the process efficiency. The introduction of Eud on the sets lead to significant losses during the whole production process.

Table 3: Yield of production of PMMA and PMMA-Eud after lyophilisation (n= 6)

Nanoparticle Formulation	Yield of production (%) (Mean ± SD)
PMMA (100)	97.76 ± 0.02
PMMA-Eud (50:50)	29.84 ± 1.35

4.2 Psychochemical Characterization

4.2.1 Particle Size Analysis

Particle production comprises different steps during all the process, and this can introduce new variables transforming our fomulations. For that reason, it is important to assure accuracy and quality, from each produced batch, characterize the NPs distribution size in cell studies. Concerning all these factors, size measurements were assessed in all the key steps of the NPs production. In figure 15, the layout presents the relationship between the production steps involved in NPs synthesis and how they can provoke size variation on particle sizes. After the

emulsification process and solvent evaporation, measurements indicate heterogeneous populations with different sizes from both sets. PMMA-Eud indicates lower values when compared to PMMA sets, but with evident fluctuations in standard deviation values.

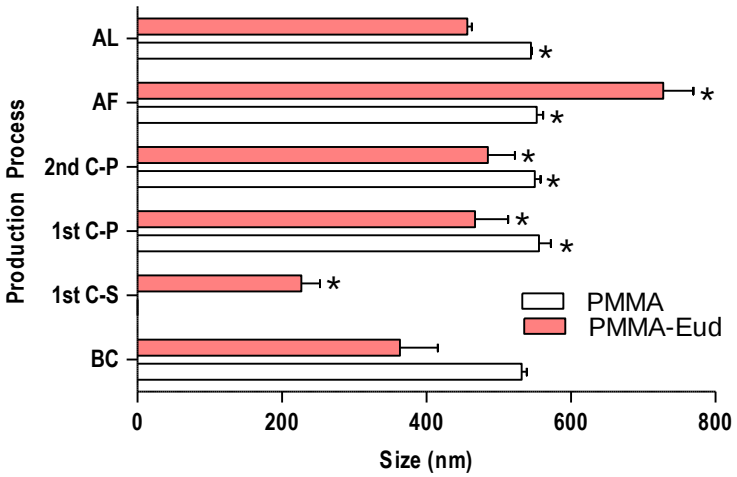

Production Step	BC	1st C-S	1st C-P	2nd C-P	AF	AL
PMMA (nm) $(\bar{x} \pm \mathbf{SD})$	532±6.8	0	556±16.3	550±8.2	552±9.0	545±0.8
PMMA-Eud (nm) $(\bar{x} \pm \mathbf{SD})$	364±52.5	227±25.8	467±45.8	485±37.2	721±41.6	456±6.2

*Figure 15: Production phases and its influence in size range distribution of NPs sets. Values presented (Mean ± SD) refer to d(0.5) (n=3). "BC" = Before Centrifugation; "1st C-S" = after First Centrifugation-Supernatant; "1st C-P" = after First Centrifugation-Pellet; "2nd C-P" = after Second Centrifugation-Pellet"; "AF" = After Freezing; "AL" = After Lyophilisation. * is referred as significantly different from the BC process. Values are presented by Mean ± SD (nm).*

Measurements were also carried out following centrifugation. NPs size on the supernatant, and on the pellet after homogenization were also determined. A prominent difference is the fact that in PMMA batches, any supernatant was able to fill in the obscuration setup. For that reason, it was not possible to measure it. The supernatant was limpid. The homogenized pellet indicates an expected size range, with slight variations regarding the previous measurement. On the opposite, PMMA-Eud presented an opaque supernatant that was easily measured. The mean value obtained was 227 ± 25.8 nm. For the homogenized pellet, the size range was 467 ± 45.8. The average values indicate that smaller particles are present in the supernatant and the larger ones are on the pellet. The second washing step showed similar particle sizes. Besides, PMMA-Eud presented a clarified supernatant that wasn't read by the Laser Diffraction. Samples were then submitted to a freezing process, an essential step for lyophilisation. Although, this sudden variation in temperature may affect NPs characteristics.

Sizes were assessed for both sets. Regarding PMMA, values remained similar to the previous one. PMMA-Eud demonstrates significant differences, increasing size values up to 721 ± 41.6 nm. In these batches, other measurements were carried out, using ultrasounds (80%) incorporated in the Laser Diffraction, during 10 minutes. The obtained result was 459 ± 1.4 nm, a much more comparable size range.

After the lyophilisation process, the powders were reconstituted in MiliQH_2O, homogenized and measured. Values obtained represent the size distribution that the cells will be exposed. PMMA-Eud with lower sizes, but still comparable to PMMA sizes range. All variables were analysed using a One-way ANOVA and Post-hoc Tukey's Multiple Comparison Test. When compared with "Before Centrifugation", PMMA values were significantly different in all conditions, except for the lyophilisation process. PMMA-Eud presented all values significantly different from "Before Centrifugation" situation.

NPs batches are now characterized regarding the size range. Although, there's still one important question to do: in which conditions, both NPs will be exposed, during the cellular assays? When *in vitro* assays are performed, it is important to mimic the real cellular environment. For that reason, all experiments were conducted at 37ºC, 5%CO_2 and with a complete medium composed of essential nutrients, vitamins and other important elements for cell growth and development. These differences in temperature and medium composition could induce size alterations on NPs. Concerning this, the size distribution of both sets of NPs were assessed in cellular assays environment. As resumed in figure 16, batches were measured before start the incubation ("BI"), where NPs were in a MiliQH_2O homogenized solution at RT (final concentration of 20 mg/mL). After that, and keeping the same concentration, NPs were incubated with complete culture medium for MG-63 (RPMI 1640; 10% FBSi; and L-Glutamine) during two endpoints: 1 hour and 24 hours).

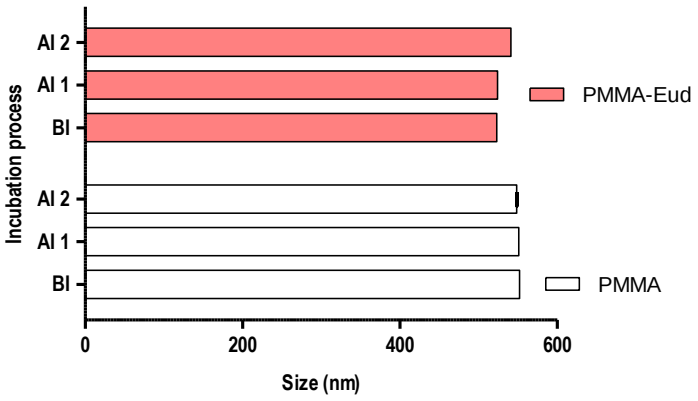

Figure 16: Incubation process and the effects on size distribution (n=3). "BI" = Before Incubation; "AI 1" = After 1 hour of incubation; "AI 2" = After 24 hours of incubation.

Standard deviation values were very low indicating homogenous size values, and reliable results.

4.2.2 Surface Charge

Surface charge is another key factor involved in NP's-cell interactions. Therefore, it was evaluated by zeta potential (mV) in different medium conditions. PMMA and PMMA-Eud sets were dispersed in MiliQH_2O and complete medium for the osteoblasts cell line. The obtained results are displayed in Table 4. Values are present as Mean ± SD.

Table 4: Surface charge of NPs dispersed in different medium composition (n=3 of the same batch).

	Zeta potential (mV) (Mean ± SD)	
Nanoparticle Formulation	MiliQH_2O	Complete Medium
PMMA	-22 ± 1	-10 ± 1
PMMA-Eud	45 ± 1	-30 ± 1

Complete medium induces alterations on both NPs surface charge. Complete medium, as already referred, is a complex mixture of compounds, all of them possible candidates to interact with reactive surfaces of NPs. In its "native" state, PMMA is strongly anionic, and PMMA-Eud is strongly cationic. Once the medium is added, PMMA-Eud goes from strongly positive to strongly negative surface charge. For PMMA, the complete medium tends to neutralise those values reducing it from -22 mV to -10 mV.

Regarding surface charge and size distribution measurements, it was possible to define the intrinsic physicochemical properties of each formulation in different medium composition and temperature. However, establishing NPs features on similar cell assay conditions, were the most important ones. When cells are exposed to PMMA, will interact with 549 nm NP and with a surface charge of -10 mV. For the PMMA-Eud NP's, size values are at 541 nm, with a surface charge of -30 mV.

4.2.3 Morphology

To analyse the morphology and agglomerate/aggregate formation, NPs were submitted to SEM analysis. Two different conditions were evaluated: each NP was dispersed in dH_2O (figure 17) and incubated for 3 hours with undifferentiated MG-63 cells supplemented with complete medium (37ºC, 5% CO_2) (figure 19).

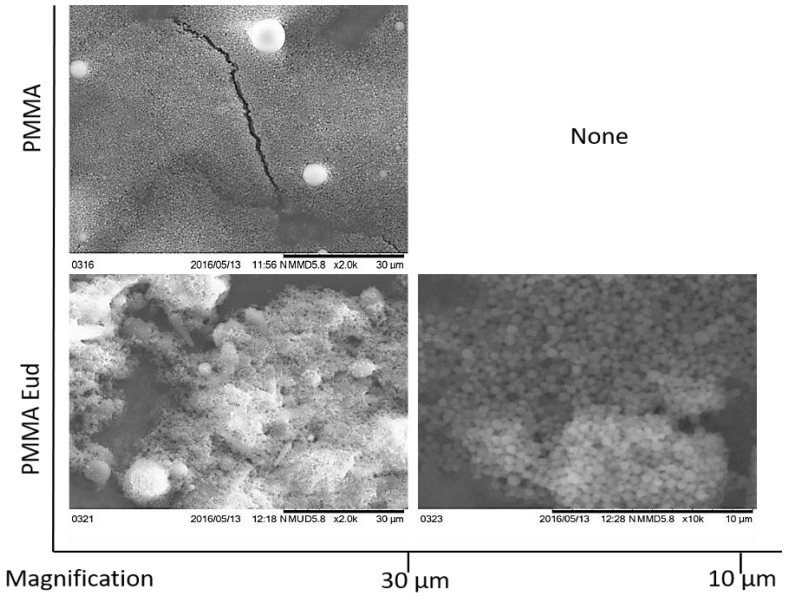

Figure 17: NPs dispersed in dH_2O.

PMMA image shows a levelled and a homogenous subset of NPs. Due to the high concentration used, NPs seems to have formed a film under the surface of carbon adhesive used to analyse the samples on SEM. PMMA-Eud on the other hand, exhibit a confused structure, impossible to define any spherical format of NP's, one of our goals for particle production. A scale up was definitely necessary to understand what those undefined bulks were. Using a 10.000x magnification, small spheres emerge from complex structures, similarly to those obtained in PMMA, but with irregular levels. Measurements were performed to record NPs size ranges on that assembly. Figure 18 shows three executed measurements (583 nm, 425 nm and 506 nm) confirming that particles morphology were kept as so as their size values. Agglomerates seem possible to be formed in PMMA-Eud batches, creating different particle populations. For PMMA, aggregate/agglomerate formation was not verified, although, rarely bigger and undefined structures appeared.

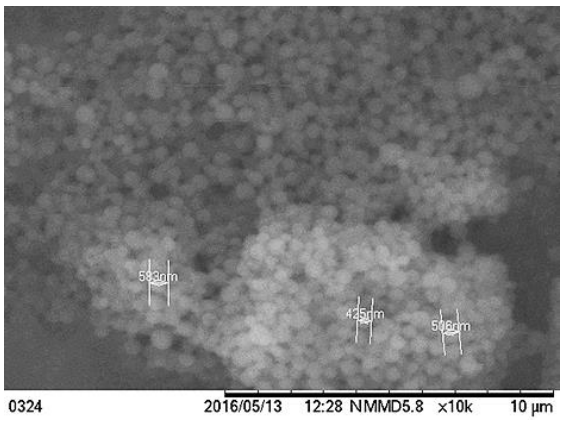

Figure 18: Size measurement of PMMA-Eud dispersed in dH_2O.

Undifferentiated MG-63 were exposed to PMMA and PMMA-Eud for 3 hours at 37ºC, 5% CO_2, (final concentration of 5 mg/mL). Results were displayed in figure 19. The reduction in final concentration was notorious in PMMA batches since particles did not form any film on the surface. PMMA-Eud presented the same bulk morphology despite the reduced concentration. The bigger spherical structures that appear in images of both NPs were measured, and the obtained values were 14,6 µm and 14 µm respectively. For that reason, they were distinguished as cells. Another mutual observable effect is the film formation over the cells. Both NPs seems to cover the cell surface and interactions are likely to occur.

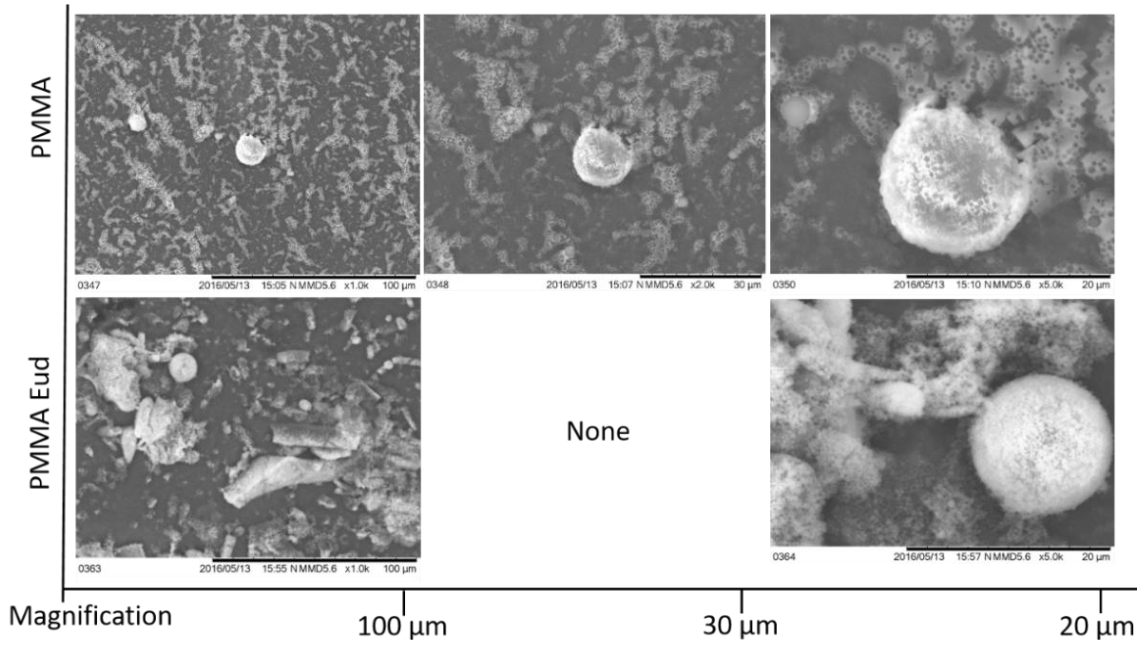

Figure 19: NPs incubated for 3 hours with undifferentiated MG-63.

4.3 Cellular Assays

In vitro cell assays represent a valuable part of this work. The biosafety evaluation of PMMA and PMMA-Eud NPs were performed in a normal and differentiated human osteoblast cell line (MG-63).

4.3.1 Cell culture

Handling with cell cultures provides the ability to recognise cell morphology and determine its cell cycle duration. Each cell type has unique characteristics, and during this work, that was confirmed. Figure 20, illustrate a cellular arrangement in normal MG-63 culture conditions, in a subconfluence state. They are adherent, forming a monolayer in tissue culture flasks, and present a lengthened structure, not affected or inhibited by another cell contact.

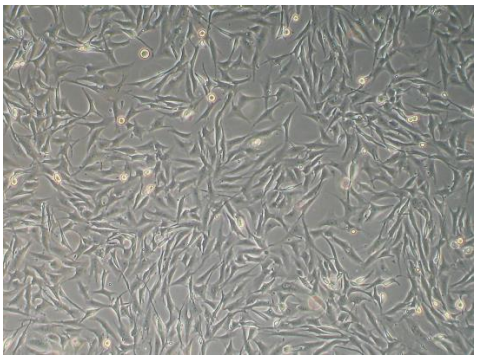

Figure 20: Normal MG-63 in subconfluence. Magnification 40x.

Normal MG-63 was cultured under differentiation medium conditions, during 72 hours. When time was reached, MG-63 became differentiated. By optical microscopy, was almost indistinguishable the external morphology between normal and undifferentiated osteoblasts. Figure 21 displays the results of a five-day experience between differentiated MG-63 and undifferentiated MG-63. Cultures had the same passage, were plated at the same density and incubated in the same conditions.

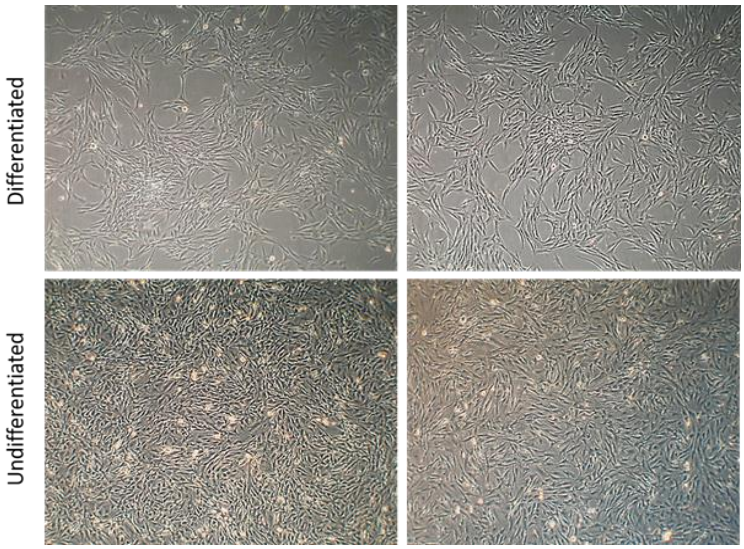

Figure 21: Cell culture of normal and differentiated MG-63 during five days. Magnification: 40x.

After five days, the undifferentiated MG-63 represents 100% confluence and may be no longer viable. The culture medium is already oxidised without nutrients to assure cell growth and development. On the opposite, differentiated MG-63 are in a subconfluence state, presenting a different cellular organisation with new arrangements. Differentiated MG-63 presents a delay on cell cycle concerning to the undifferentiated ones.

4.3.2 Differentiation Assays

To confirm cellular differentiation through specific medium components, two parameters were evaluated: AP activity and calcium deposition. As a negative control, an embryonic kidney cell line (HEK293T) was used.

4.3.2.1 AP Activity

The AP activity was assessed during 180 minutes with time intervals of 1 minute for each measurement. Data from 8 replicates were presented in figure 22. Represented in blue lines is the differentiated MG-63, the red lines represent the undifferentiated MG-63, and green lines stand in the HEK293T cell line.

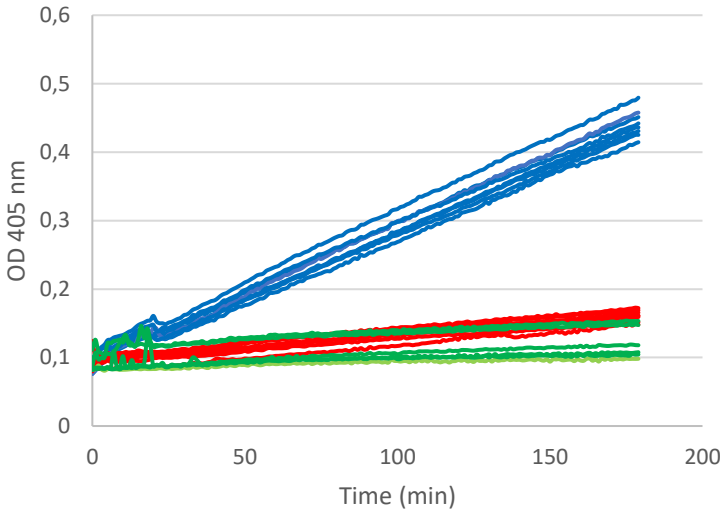

Figure 22: Absorbance values during 180 minutes. In blue are represented differentiated MG-63, in red undifferentiated MG-63, and green are represent the HEK293T. Values are in Absorbance Units (UA)/minute.

Is notorious that the differentiated MG-63 has contrasting behaviour compared with the other studied situations. Differentiated MG-63 presented a much higher Optical Density (OD) values, during the time explored and revealed a positive and linear correlation between OD 405 nm and time. By the undifferentiated osteoblasts and the HEK293T comparison, the first one represents slightly but higher absorbance values. The OD values on HEK293T were quite low (almost 0) indicating a good negative control for the experiment. The slope calculation as the correlation coefficient (R^2) was also appraised, but in this case (HEK293T), values were not considered since they were extremely low. For that reason, HEK293T was not used for protein quantification, but only for assay validation. Using known concentrations of BSA protein and measuring the values obtained in OD, a calibration curve was constructed to estimate the total amount of protein present in differentiated and undifferentiated MG-63 (annex 1).

The estimated values for the AP present on cell lysates were: differentiated MG-63 0.056 ± 0.003 AU/min.μg^{-1} of protein (AU: Absorbance units), and normal MG-63 0.005 ± 0.001 AU/min.μg^{-1} protein. Analysing these values, the present amount of AP on the osteoblasts cultured under differentiation medium conditions is almost ten times higher to the osteoblasts cultured under normal conditions.

4.3.2.2 Calcium deposition

Calcium deposition is another important biomarker for characterization on human osteoblasts. For that reason, it was used to confirm differentiation on MG-63, induced by differentiation medium components. Using the Alizarin Red it is possible to specifically stain calcium deposits into a bright orange precipitate formation, and its fluorescence measured. Using the BCA assay in the same conditions described above, calcium deposition was determined to compare the normal and differentiated MG-63 and using the HEK293T as a negative control.

The measurements values obtained in differentiated osteoblasts were higher than from those achieved in normal osteoblasts (table 5 and annex 1). Although, the difference between them are not very significant. The HEK293T presented extremely low values, and for that reason, it was not used for the quantification.

Table 5: Absorbance values in fluorescence units by differentiated and normal MG-63 and HEK293T cell line. For HEK293T, this evaluation was Not Applicable (N.A.).

Cell line	Fluoresce Units (UF) (Abs: 405 nm)	UF/µg of protein
Differentiated MG-63	1713 ± 544	22490 ± 3439
Undifferentiated MG-63	1505 ± 249	20306 ± 3428
HEK293T	436 ± 50	N.A.

4.3.4 Uptake Assay

The uptake assay constitutes the first step of the toxicological evaluation of PMMA and PMMA-Eud. The distinction between internalised and non-internalized NPs is extremely relevant to understand the results of cytotoxicity and genotoxicity assays. The internalisation method was performed only in differentiated MG-63 since a previous work has already confirmed the internalisation in normal MG-63 (Graça 2014). To quantify the internalised NPs a BCA test was also used, as described above (annex A).

Results are presented in figure 23 were both NPs were successfully internalized. For PMMA and PMMA-Eud, the uptake by differentiated osteoblasts seems to be concentration-dependent, higher NPs concentrations induce a higher internalization. On the other hand, PMMA sets were more easily internalized in both conditions when comparing to PMMA-Eud NP's.

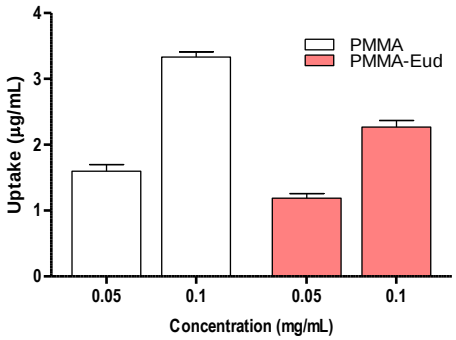

Figure 23: Uptake assay considering two tested concentrations of PMMA and PMMA-Eud.

4.3.4.1 Fluorescence Microscopy

Optical analysis recurring to fluorescence microscopy techniques was executed using the Coumarin-6 loaded NPs in the same assay conditions described for the uptake assay. Using a multi-staining procedure, it was possible to distinguish the nuclear and cytoplasmic compartment in the observed cells. The loaded NPs with a green fluorescence were also easily distinguishable in the cells. Table 6 present the acquired images. By the optical analysis, was possible to confirm some of the obtained results in the uptake assay. NPs internalisation seems directly proportional to the tested concentration for both sets. Concerning the different cellular compartments, NPs doesn't suggest to be situated in the nuclear compartment, although this is only a hypothetical statement. In contrast, this assay was not relevant to detect differences between PMMA and PMMA-Eud internalisation as reported on the uptake assay.

Table 6: Imagens (40x) from fluorescence microscopy. Columns indicate the singular labelled cells components, and the Coumarin-6 loaded nanoparticles used for this assay. The last column set all images together.

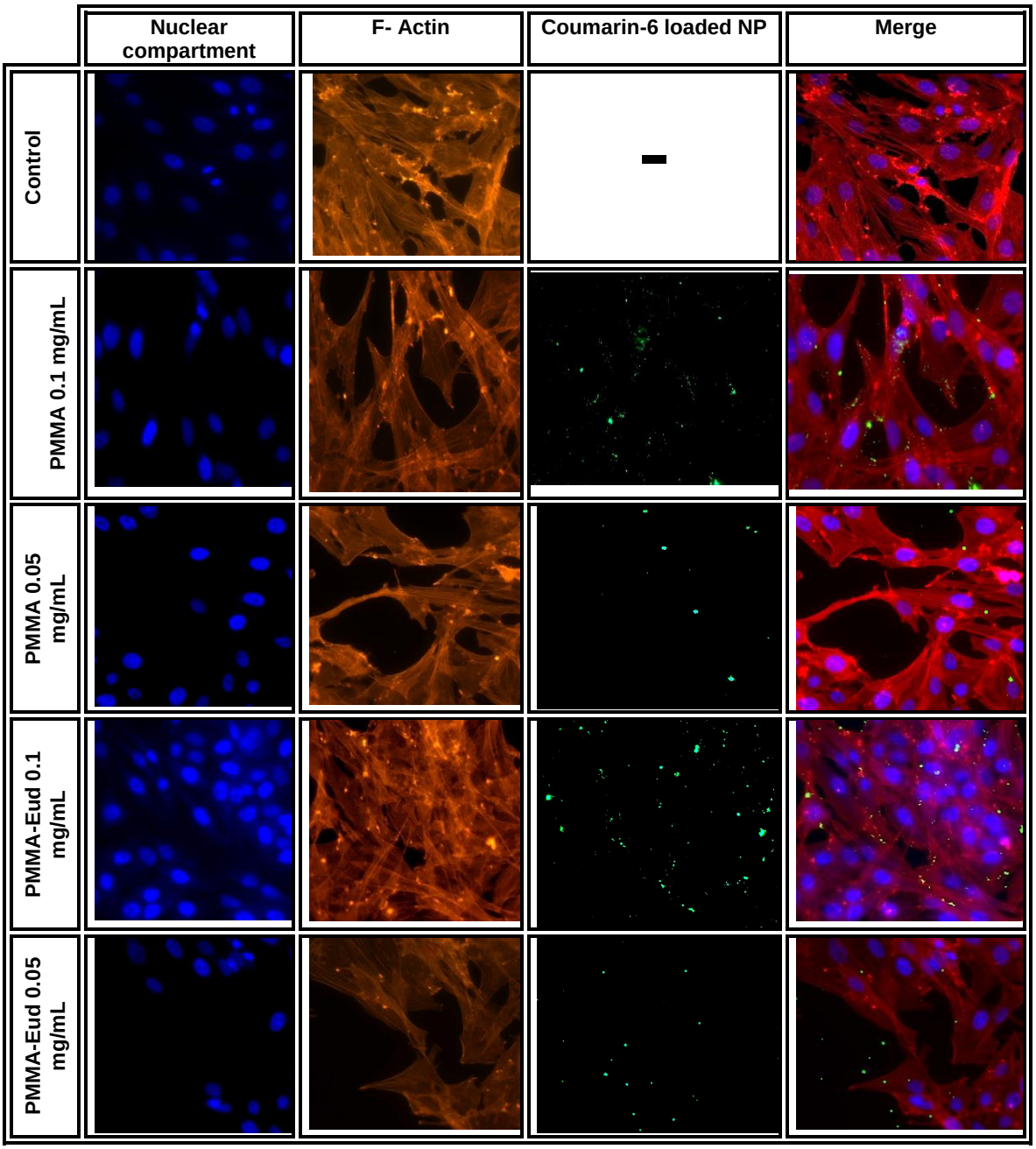

4.3.5 Cytotoxicity and oxidative stress induction

Cytotoxicity was evaluated in this work through the MTT assay, while the ability to generate ROS was assessed by the H_2DCFDA assay. The first assay was explored in differentiated and undifferentiated MG-63 cells while the second one was only performed in differentiated MG-63 cells, since a previous study had already reported those results for undifferentiated MG-63 cells (Graça 2014).

Since the MTT assay relies on spectrophotometric readings, NPs can interfere with the reagents leading to misconceived results (Collins et al. 2016). To exclude that effect from our results, a preliminary test was executed in the defined concentration range with MTT. Any interactions were recorded by absorbance readings, although particles deposition on well-plates were quite evident. These findings can introduce interferences on the obtained data and increase the absorbance values, since the NPs deposition can cause a higher opacity in the solution.

Figures 24 and 25 graphically present the results obtained for cell viability following 24 and 64 hours (undifferentiated and differentiated) MG-63 cells exposure to both NP formulations. The shortest time point explored did not show any significant decrease in cell viability neither for normal MG-63 nor for the undifferentiated ones. In fact, even an increase in cell viability was observed for 0.1 and 0.5 mg/mL of PMMA-Eud. In contrast, some cytotoxicity was noted after 64 hours incubation with NPs. The viability of MG-63 cells cultured under normal medium conditions was affected by PMMA-Eud in a concentration-related manner, suffering a reduction to approximately 55%, at the highest concentration tested ($p < 0.01$). PMMA also induced significant cytotoxic effects in undifferentiated MG-63 cells, but only when exposed to 2 mg/mL and 5 mg/mL ($p = 0.001$ and $p < 0.01$, respectively). Contrasting to these results, differentiated MG-63 cells did not evidence any significant reduction of viability after 64 hours exposure to both NPs even though a slightly reduction of cell viability was noted for 64 h exposure to PMMA-Eud. SDS, was used as positive control, and was strongly lethal for differentiated and undifferentiated cells.

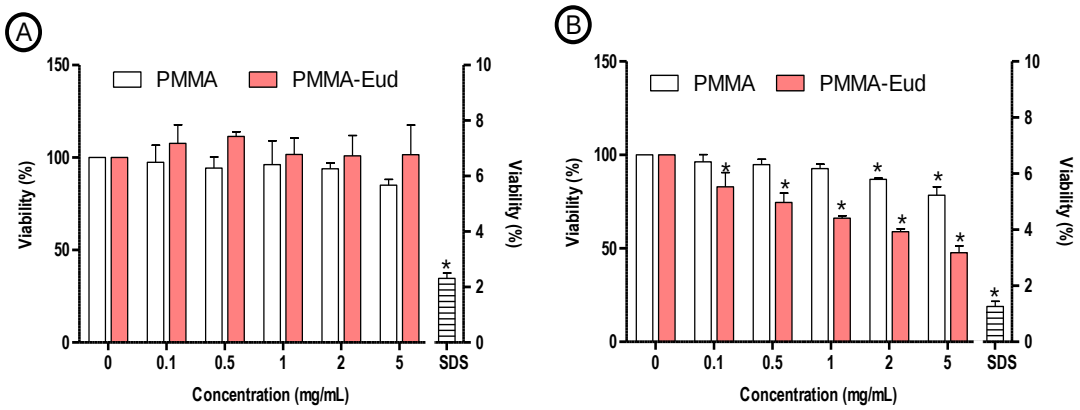

*Figure 24: Results of the viability assessment of PMMA and PMMA-Eud in undifferentiated MG-63 cells. (A) represents the data from 24 hours exposure and (B) refers to 64 hours exposure. SDS is the positive control. * significantly different from the control ($p<0.05$).*

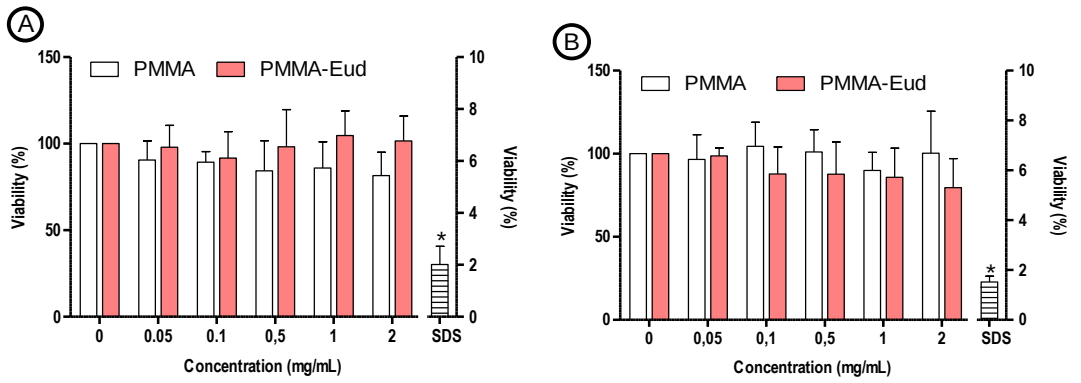

*Figure 25: Results of the viability assessment of PMMA and PMMA-Eud in differentiated MG-63 cells. (A) represents the data from 24 hours exposure and (B) refers to 64 hours of exposure . SDS is the positive control. * significantly different from the control. (p <0.05)*

The ability of PMMA or PMMA-Eud to induce ROS production was measured after 1 and 3 hours to differentiated cells exposure (figure 26). No evidence of significant ROS induction was observed at both endpoints and for both NPs. H_2O_2, chosen as the positive control, induced an almost 100-fold increase in the RFU level as compared to untreated cells at both timepoints.

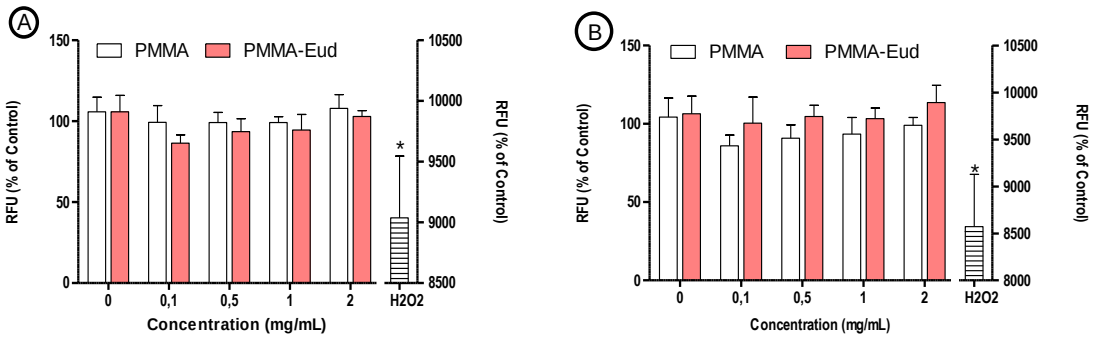

*Figure 26: ROS production by H_2DCFDA assay in differentiated cells. (A) data from 1 hour exposure and (B) data from 3 hours exposure to PMMA and PMMA-Eud. H2O2 is the positive control. * significantly different from the control (p<0.05).*

4.3.6 Genotoxicity Assessment

Genotoxicity assessment of PMMA and PMMA-Eud formulations was conducted through the characterization of direct and indirect effects at DNA and chromosome levels. CBMN assay was performed in MG-63 cultured under normal and differentiation medium conditions while the Comet assay was carried out only in undifferentiated osteoblasts.

4.3.6.1 Characterization of DNA damage by the Comet Assay

DNA damage was measured after cells exposure to PMMA and PMMA-Eud during 3 and 24 hours (figures 27 and 28). As already described, the modified version of the Comet Assay using the FPG enzyme was also included, to additionally evaluate oxidative DNA damage that may be generated by these NPs. The level of DNA lesions was significantly raised by the treatment with PMMA and PMMA-Eud for 3h, at all concentrations tested. Although a concentration-dependent increase in the level of DNA damage was noted, the data could not be adequately fitted to any mathematical function. PMMA-Eud formulations revealed to be slightly more genotoxic comparatively to PMMA for the several concentrations tested. The use of FPG to reveal oxidized bases did not show significant increases in the level of DNA damage when compared to the condition without this enzyme. The highest concentration of 5 mg/mL led to significant NP deposition over nucleoids disabling their analysis. For that reason, the results correspondent to that concentration of PMMA-Eud were not presented at both exposure times.

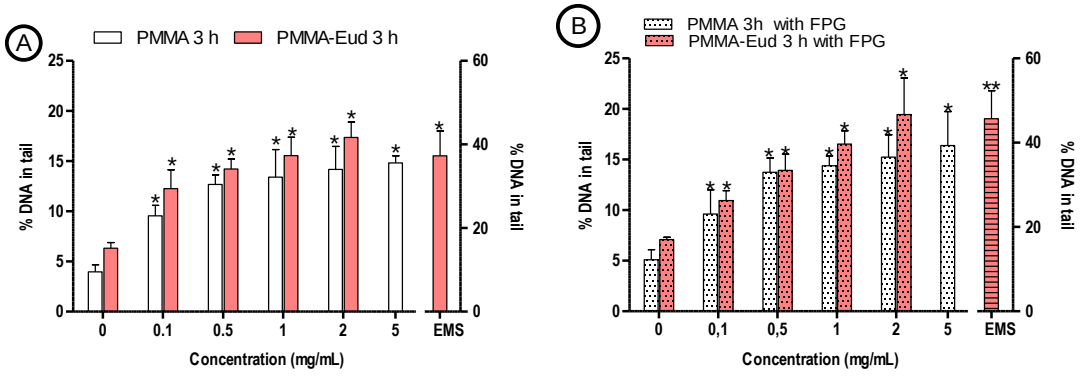

*Figure 27: Results of the Comet Assay for undifferentiated MG-63 cells after 3 hours exposure to PMMA and PMMA-Eud. (A) represents the conventional assay, and (B) the assay with FPG. EMS was used as the positive control. * significantly different from the control ($p<0.05$) and ** significantly different from EMS without FPG.*

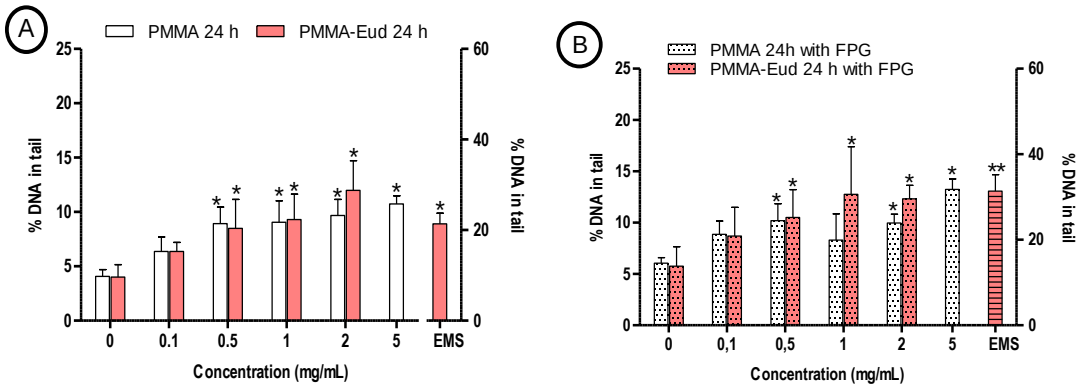

*Figure 28: Results of the Comet Assay for undifferentiated MG-63 cells after 24 hours exposure to PMMA and PMMA-Eud. (A) represents the conventional assay, and (B) the assay with FPG. EMS was used as a positive control. * significantly different from the control (p<0.05) and ** significantly different from EMS without FPG.*

After 24 hours, MG-36 cells were slightly less affected by the toxic effects of PMMA or PMMA-Eud. Using the Student's t-test to compare the % of DNA in tail obtained after 3 and 24 hours of NPs exposure, in all concentrations it was found values significantly different ($p<0.05$). The reduction of the percentage of DNA in tail observed after 24 hours, was also evaluated (annex 3). In long-term exposure, the percentage of DNA in tail for PMMA NPs reduced almost 30% and PMMA-Eud NPs reduced the DNA damage in 40%. The lowest concentration of both NP did not induce a significant increase in DNA damage as compared to the control (PMMA: $p=0.22$; PMMA-Eud: $p=0.56$). However, all the other tested concentrations induced a significant level of DNA damage ($p<0.02$). Another important observation was the results obtained for the modified Comet Assay. None of the concentrations tested presented differences before and after the FPG treatment suggesting that The NPs did not induced the formation of oxidised bases. However, differences between treated and untreated cells were observed ($p<0.05$) in the same conditions as the cultures analysed in the conventional Comet assay. EMS was used as positive control, presenting significant increases of DNA breaks comparatively to the control for all performed assays, as expected.

4.3.6.2 Characterization of chromosome alterations by the CBMN Assay

Damage at the chromosome level was evaluated considering a long-term exposure. Differentiated and undifferentiated MG-63 cells were exposed to the NP formulations under test during 64 hours. The results are displayed in figures 29, 30 and 31. Concerning the frequency of micronucleated cells (MNBNC) per 1000 binucleated cells (BNC), no significant differences were observed between treated and control cells, independently of their differentiation status. MMC was chosen as a positive control, displaying significant differences from the untreated cultures.

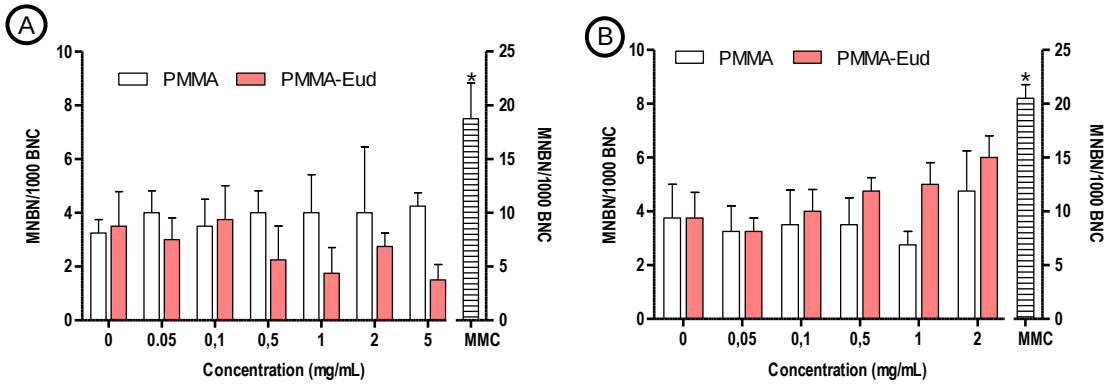

*Figure 29: Micronucleated binucleated cells (MNBN) frequency per 1000 BNC cells. (A) represents the output obtained in undifferentiated MG-63 cells, and (B) represents the output from the assay performed with differentiated MG-63 cells. MMC was used as a positive control. * significantly different from the control.*

The CBMN assay can also provide information about cytotoxic effects by the analysis of proliferation and replication indexes.

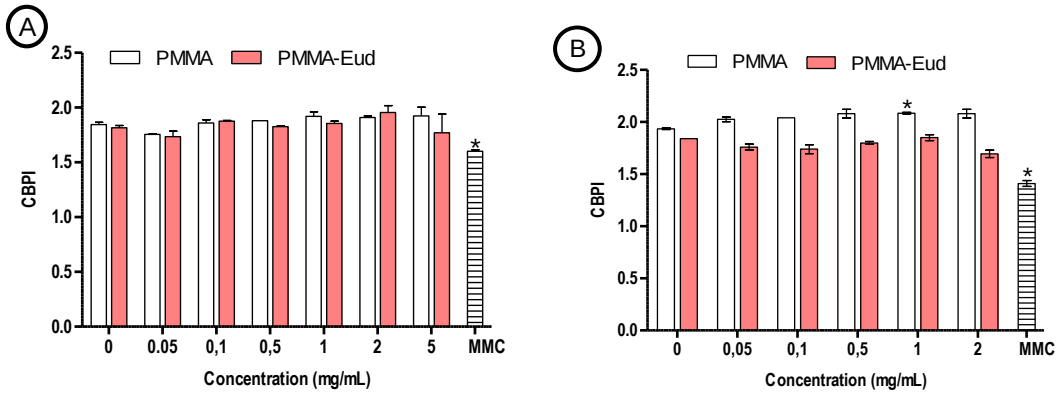

*Figure 30: CBPI estimated for undifferentiated (A) and differentiated (B) MG-63cells after treatment with PMMA and PMMA-Eud for 64h. MMC was used as a positive control. * significantly different from the control.*

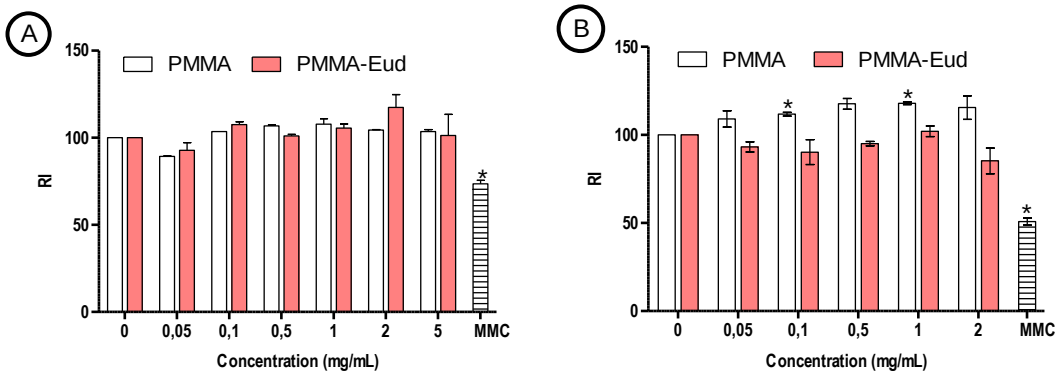

*Figure 31: RI estimated for undifferentiated (A) and differentiated (B) MG-63 cells. MMC was used as a positive control. * is significantly different from the control.*

By the CBPI and the RI analysis, alterations on the cell cycle progression and on the cells capacity to enter mitosis, respectively, were not altered by the treatment with PMMA-Eud. Likewise, PMMA did not influence the osteoblasts cultured under normal conditions. However, the cell progression through the cycle of the differentiated osteoblasts seems to be slightly stimulated by PMMA, being the difference significant for the concentration of 1 mg/mL ($p=0.04$). This NP was also able to stimulate differentiated osteoblast to divide by mitosis, particularly at the concentrations of 1 mg/mL and 0.1 mg/mL ($p=0.02$ and $p=0.04$, respectively).

Another information that came up from the CBMN assay was that the NP concentration can affect the data quality. In fact, the PMMA-Eud NPs tended to cover cells at the concentration of 5 mg/mL concentration, which prevented micronuclei scoring (only 411 binucleated cells were evaluated in 1000 cells). Cellular agglomerates can also be formed, at these high concentrations, which decreases the preparation quality for data analysis (figure 32). Given that these observations were obtained with undifferentiated MG-63 cells, the 5 mg/mL dose was not assayed in differentiated MG-63 cells and for none of the NP formulations.

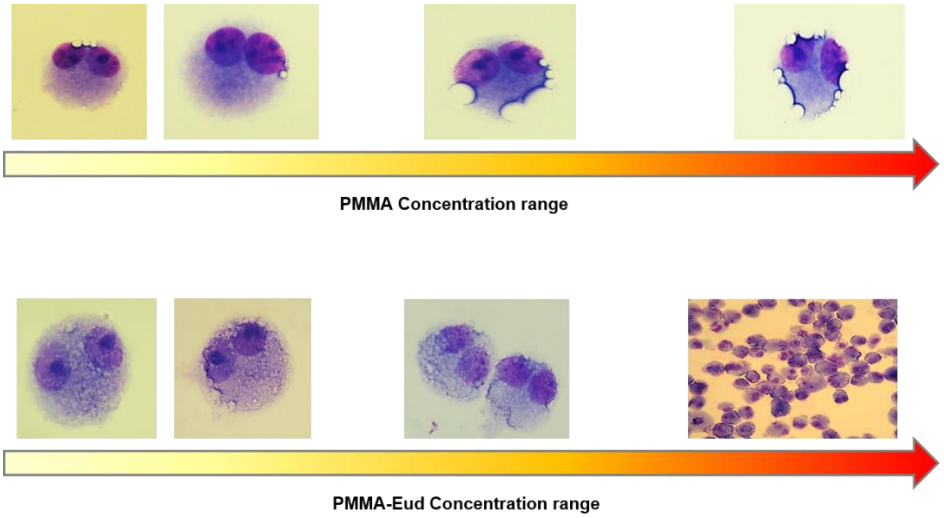

Figure 32: Undifferentiated MG-63 are represented in the studied concentrations. Images acquired with 100x and 40x amplification.

Depicted in figure 32, is the main effects of high levels of PMMA and PMMA-Eud on cell aspect. Both NPs can introduce deleterious effects on cell scores since most of the times, the main nucleus and cell boundaries remained unclear. These effects are concentrate-dependent, indicating that the explored doses should be adjusted in order to obtain more accurate results.

5. Discussion

5.1 Nanoparticles Production

Polymer nanotechnologies had already proved to be an important benchmark in our society. Polymers as long chains of repeating structural units have gained a lot of interest as drug delivery systems and are an actual subject of today. Their distinct properties held by the nanoscale, allow an enhancement of pharmacokinetics and biodistribution of drugs in the target tissue. However, these characteristics are intimately connected to micro and nanoparticles production methodology. Polymeric NPs can be prepared by direct polymerization of monomer units or by pre-formed polymer techniques (Vauthier & Bouchemal 2009). Each process encompasses its own advantages and disadvantages. PMMA NPs were already being produced through different methods, but the most frequent one is the SESE, and for that reason it was also used in this work to obtain PMMA and PMMA-Eud formulations.

SESE technology presents some objections related to the use of organic solvents and surfactant agents during the nanoparticles formation. These solvents should be removed at the end of the process to reduce cytotoxic effects. DCM, a class 2 solvent according to ICH regulation, have a limited residual concentration in which it doesn't present adverse effects to patients. The maximum allowed concentration of this compound is 600 ppm (ICH 2011). The rationalized used of DCM is held by its high volatility and lower residual solvent rates after NPs purification and lyophilisation steps. Alternatives to DCM, including ethyl acetate or propanone have already been tried, but with considerable drawbacks. DCM still represents the best option to assure better yields of production. Furthermore, Florindo et. al (2010) reported DCM residue (% w/w) values, less than 10 ppm in freeze-dried polymeric NPs, assessed by NMR spectroscopy. Furthermore, the optimized washing steps used in this work also helped to remove some chemical depositions in nanoparticles.

In another perspective, PVA is also added as a surfactant to reduce surface tension and to stabilize the oil-in-water emulsion process. Ionic and anionic surfactants may be used in the production of polymeric particles. PVA, SDS, poly(ethylene oxide) are some of the most used surfactants in chemical synthesis, and that solvent selection/concentration will directly affect NPs features. For instance, ionic surfactants introduce a positive charge to NP surface mediating the internalization process. PVA molecular weight also seems to had impact on NPs stabilization (Hocherl et al. 2012). Techniques as surfactant-free emulsion polymerization have also successfully produced PMMA NPs without PVA or any stabilising agent. However, polymerization is carried out by gamma irradiation (500 Krads, γ rays) or by a chemical initiator such potassium peroxodisulphate. Thus, it also suggested other possible outcomes or concerns.

When comparing SESE to other available methodologies to produce PMMA and PMMA-Eud NPs, the advantages include a cost-effective, fast and easy scale-up method. Low polydispersity of the particles is also expected. The disadvantages comprise the toxicological issues described above. A previous work developed by our group, have studied and optimized PMMA and PMMA-Eud NPs production process considering the restrictions held by DCM and PVA appliance (Graça 2014). It was concluded that the lowest NPs size that could be obtained with SESE method was 500 nm. As such, the same methodological conditions were chosen in this work to carry out the NPs production.

Results for the yield of production (table 3) obtained in this study are comparable to others reported by Graça et al. (2014) (Annex 4) or Bettencourt et al. (2010). Recovering 98% of the PMMA polymer after lyophilisation process, confirm that the used method is reliable to produce 500 nm PMMA NPs. PMMA-Eud yields were considerably different from PMMA since only 30% of the polymers were recovered. It was harder to obtain PMMA-Eud NPs due to the increment of Eud that has dramatically reduced the process efficiency. Eudragit ® is a synthetic mixture of copolymers of PMMA, and since is industrially produced, the brand has diverse reproducible forms. Thakral et al. (2013) performed deep physicochemical characterization of several forms of Eudragit ® including Eud itself. Authors concluded that when solubility profiles pH dependent or independent, is medium-low the polymer tends to form a film. That film can be flexible or soft, and the addition of methacrylate ester copolymer leads to a more permeable film. Since the used Eudragit ® form presents this methacrylate ester enhancement in its chemical composition, this can provide an explanation to the lower production rates of PMMA-Eud NPs. After the emulsification process, Eud had formed a film in the glass flask. The purification steps showed a less stable pellet comparing to those obtained with PMMA formulation. Furthermore, Eud polymer induced the adhesion of NPs in the glass and to the plastic of centrifugal tubes due to the proved permeability of films experienced in these polymers.

PMMA is systematically described as a hydrophobic polymer, and despite the high yield of production, it still affects the drug release profiles and the drug retention inside the nanoparticles. Strategies to reduce hydrophobicity of PMMA include surface functionalization or incorporating hydrophilic polymers in the formulations such as Eud. The reduced yield of production can lead us to considerate other strategies. Polyethylene glycol (PEG) is often applied in drug delivery systems as a modifying surface polymer, it is an FDA approved material, and highly soluble in water. For many reasons, PEGylation can be considered in future works (Veronese & Pasut 2005).

5.2 Physicochemical characterization

As an integrant part of any nanotoxicological study, a physicochemical characterization follows the nanoparticles production. Understanding how NPs interact with biological barriers in a physiological environment provides valuable information to understand and predict the toxicological profile of the nanomaterials.

By several authors, particles size constitutes the most important feature at the nanoscale. It has a significant impact on translocation across cell barriers, on biodistribution, and on clearance mechanisms. Assess NPs size is always mandatory to physicochemical depiction. LS was used to assess size values in all production steps included in PMMA and PMMA-Eud production, and in incubation tests. Another key factor to evaluate NPs size or another physicochemical indicator is choose a correct dispersant medium. In a first analysis, NPs should be dispersed in the simplest medium as possible not affecting NPs solubility but in a way, that it doesn't introduce any interference compounds, compromising the results (European-Scientific-Committee 2009). In that perspective, NPs sizes were assess using MiliQH_2O, and those values were then compared to those obtained in complete culture medium.

In the different production processes results of size measurements (figure 15) presented heterogeneous values not only between both NPs sets, but also in each production step. PMMA size values were consistent along the process and the size range obtained after the lyophilisation were not significantly different from those obtained after the solvent evaporation process (figure 15: "before centrifugation"). As already mentioned the obtained pellet was also quite stable, and few losses were associated. In PMMA-Eud, differences were more pronounced, and the obtained data were in all conditions, significantly different ($p < 0.01$) from the size distibution values obatined after the solvent evaporation process. In that condition, values demonstrate a heterogenous population with high deviation values (figure 15, "before centrifugation"). NPs size measurements on the supernatants indicate that the first purification step was important to remove smaller particles since the pellet presented values around 500 nm. Being able to measure the supernatant can also justify some of the associated losses during the PMMA-Eud production and the low yield of production values (table 3). Those NPs weren't recovered. After particles freezing, great differences were observed. Decreasing the temperature have promoted a new assembly of the NPs and reduced the solution stability. Using an incorporated ultrasound system in PMMA-Eud samples promoted a shift in size values from 721±41.6 nm to 459±1.4 nm. This indicates a presence of reversible clusters on PMMA-Eud formulations. Low temperature promotes *in situ* agglomeration states based on weak chemical interactions (Sokolov et al. 2015). Thus, it can form a bimodal population, incremented with NPs that are larger than the colloidal size. Although the whole process seems to be reversible, and the aim of the production was achieved in both formulations. Exploring the NPs sizes in cell assay conditions, demonstrated stable NP sets (figure 16) without significant differences in size values from NPs before the

incubation processes. Increasing the temperature to 37ºC didn't seem to affect NPs behaviour regarding size range, as well as the complete medium for osteoblasts.

Surface charge reveals itself as especially relevant property to understand the interactions between NPs surface and cellular entities. It compromises the uptake mechanism, subcellular localizations and the ability to trigger toxic events (Sutariya & Pathak 2015). Charge is also a stability factor of NPs in different solvents. Electrophoretic mobility of NPs were measured by zeta potential using different dispersant mediums. Results obtained in MiliQH_2O for PMMA and PMMA-Eud (table 4) were comparable to other reported studies (Graça 2014; Hocherl et al. 2012; Ferreira 2015). Theoretically, PMMA-Eud has a positive surface charge due to the quaternary ammonium groups in its composition, which is confirmed by the obtained data. When NPs are dispersed in a complete medium, variations in surface charge are observed in both formulations. PMMA-Eud changes to strongly positive to strongly negative charges, and PMMA from strongly negative to neutral. Complete medium is composed of several serum proteins used as a nutrient source of cultured cells. When NPs are exposed to these compounds, proteins adsorb onto NP surface forming a protein "corona". This event was also observed in a great variety of NPs including silver gold, silica and polymers. A reported study by Fleisher et al (2014) have observed that initially cationic polystyrene NPs (ζ = +20 mV) became anionic (ζ = -19 mV), and initially anionic NPs (ζ = -31 mV) showed an increase in zeta potential to - 27 mV. These results can be comparable from those obtained in this work since the same happened in PMMA and PMMA-Eud. Fleisher et al. (2014), in that same study, also analysed the corona proteins and conclude that when FBS is present in the surrounding medium, BSA is the main protein adsorbed on the NP surface. Albumin can be recognized as a negatively charged protein committing the surface charge values of NPs and explaining the obtained values.

Morphology and aggregate/agglomerate formation were analysed by SEM technology (figures 17, 18 and 19). Shape-dependent toxicity has also been reported in several NPs (i.e. carbon nanotubes). Different shapes activate different endo- or phagocytose mechanisms and thus commanding the NPs fate in cellular boundaries. Results showed spherical sets for PMMA and PMMA-Eud. PMMA presented a homogenous population contrarily to PMMA-Eud were different particle assemblies were noticed. After the studies on size measurements, this result was expected since any ultrasounds were applied on both samples. On PMMA NPs, it was observed bigger spherical structures that were not recognised. One theoretical explanation for this could be the coalescence induction. Particles in suspension can collide with atoms or molecules presented in the surroundings. NPs can even collide with each other and merge during that contact to form a single and bigger particle. NPs usually coalesce to reduce their surface energy (Ingham et al. 2011), but this should be explored using different techniques in order to analyse and measure those structures. SEM also allowed to detect aggregate/agglomerates in PMMA and PMMA-Eud sets. As expected, PMMA-Eud presented large agglomerates concluding that ultrasounds or any other method that can ensure a correct homogenization and agglomerate disruption are mandatory before any cellular exposure.

5.3 Cell Assays

5.3.1 Cell differentiation

Primary cell lines provide excellent systems for the study of the normal biochemistry and cellular response to chemicals exposure. However, they have a very limited number of cell divisions with optimized culture conditions for short periods of time, and for that reason they are not always a cost-effective option. In alternative, immortalized cells or tumor-derived cells are frequently used for bioassays. For example, osteosarcoma-derived cell lines such MG-63, are commonly used as osteoblast models. Osteosarcoma cells share many features of normal human bone osteoblasts, but they also differ in many aspects, including their proliferation capacity and gene expression. To overcome these drawbacks, MG-63 cells were stimulated to differentiation for better approach human bone cells response to the NPs under study. Differentiation of "normal" MG-63 was induced by osteogenic additives addition to the culture medium: dexamethasone, ascorbic acid and β-glycerophospate. These compounds are known to induce the expression of the osteoblastic phenotype in bone cell models, shown by Park (2012). This author reported for a pre-osteoblastic cell line an in-depth study of the effects of these compounds regarding cell proliferation, differentiation/mineralisation and protein expression. In this work, differentiated MG-63 cells did not present an altered morphology when compared to "normal" MG-63 cells. This fact was also documented by Park (2012) that reported that in short-term cultures, none of the used compounds seems to affect the morphological structures of osteoblasts (figure 20). Noteworthy, a delay in cell cycle was noticed on differentiated MG-63 cells, which agrees with the current knowledge that differentiated cell lines present lower levels of proliferation when directly compared to non-differentiated cells (figure 21). This is an intrinsic characteristic of specialized tissues. It is also known that dexamethasone acts as a suppressor of the cell cycle turnover and may have impact on cell proliferation, as well (Iu et al. 2005).

The AP activity is an important biomarker to detect cellular differentiation in osteoblasts. The reaction kinetics of the differentiated cells was almost 10 times higher than that obtained for "normal" osteoblasts confirming the cells differentiation status. In fact, β-glycerophosphate has been reported as an important phosphate source for bone mineralization (Langenbach et al. 2013), and ascorbic acid is known to induce the osteoblastic differentiation by increasing the collagen accumulation (Shiga et al. 2003). The role of dexamethasone remains unclear, although it is necessary for a significant increase in the AP activity in differentiated cells (Park 2012).

It has been described that calcium deposits are formed during the process of osteoblast differentiation and thereby to further confirm MG63 cells differentiation the calcium was quantified by the alizarin red assay (table 5). Although a slight increase in calcium deposition was detected in differentiated relatively to "normal" MG-63 cells, the difference observed was not clearly distinctive. This can be due to the low duration of the assay. Once the differentiated MG-63 cell line present a delay in the cell cycle compared to the undifferentiated ones, 24 hours could not be sufficient for the cells to produce calcium deposits. Park (2012) concluded that mineralized

nodules formation is dependent on the ability of osteoblasts to form multilayered clusters. Thus, the quantification of calcium deposits in osteoblasts cultured for longer periods of time under differentiation conditions may be an interesting option. This can increase the capacity to form mineralized nodules and to distinguish the differentiation status. However, long-term use of dexamethasone was also reported to reduce mineralization, and this should be considered. Even though, additional studies are needed for an unequivocal cell characterization considering protein (i.e osteopontin, osteocalcin, transforming growth factor-beta, etc) and gene (Runx2, Osterix, etc) expression that are related to bone formation and cell specialization, by western blot (Park 2012) or polymerase chain reaction techniques (Grabowski 2015), still MG-63 cells represent a valuable cell model of bone tissue amenable to differentiation. In respect to the safety assessment of PMMA and PMMA-Eud, this cell model can be further used to study the possible impact of the NPs on the capacity of MG63 cells to differentiate in culture conditions as described by Pauksch et. al (2014).

5.3.2 Cellular uptake

When a NP is developed to act as a dynamic drug-delivery system, the uptake mechanism should be assessed, not only to evaluate the uptake efficiency of a target tissue, but also to relate putative toxic events to the level of NP internalization. Several physicochemical properties seem to affect the uptake of NPs. Among them, the size, the shape and the surface charge seems to be the most important to activate a particular internalization cellular route. The uptake is referred as a mechanism that represents a certain endocytic capacity. When this pathway becomes saturated, NPs are no longer internalized.

In this perspective, human osteoblasts under differentiation conditions were exposed to low concentrations of PMMA and PMMA-Eud. It should be pointed out that the tested NPs present distinct surface charges that may have impact on their internalization efficiency. Indeed, zeta potential values indicated that, in complete culture medium, PMMA-Eud was highly cationic whereas PMMA was a slightly anionic or neutral NP. As can be seen in figure 23, at the concentration of 0.1 mg/mL PMMA were more efficiently uptaken by cells than PMMA-Eud NPs (1 hour of incubation), but no significant differences were noticed at 0.05 mg/mL. Thus, a concentration-dependent effect was observed since the internalization of both NPs was directly proportional to the amount of available NPs;

On the other hand, during slides scoring within the CBMN assay, many NPs deposits were observed over the cells surface, which were more evident for PMMA-Eud than for PMMA (Figure 32). Fleisher et al (2014), demonstrated that cellular binding of polystyrene cationic NPs is increased when compared to anionic ones. This may happen because different cellular receptors are activated for this binding and mediate different endocytic pathways. Thus, it can be hypothesized that PMMA-Eud may be more adsorbed/attached to the cell surface than PMMA

NPs due to their positive surface charge. However, the highest adsorption to the cell surface did not correlate with a higher level of internalization of PMMA-Eud, as could have been expected. This observation indicates that cellular binding does not represent better uptake efficiency. For a better distinction between internalized and adsorbed NPs on the cell surface, TB was used as a fluorescence blocker for those NPs that did not pass through cell barriers giving false positives. After the addition of TB, fluorescence values decreased for both NPs sets (data not shown) indicating that the background signals from the extracellular NPs were quenched and the measured data was restrained to the internalized NPs.

The uptake can be further explored for a new concentration-range of NPs and to figure out when PMMA or PMMA-Eud inhibit the internalization mechanism of osteoblasts. Another interesting approach would be to assess the uptake efficiency at different incubation times. Graça (2014) (annex 4) and Horchel (2012) evaluated internalization of PMMA NPs during 24 hours. We can consider that better results can be achieved in longer periods of exposure. Nonetheless, the concentration factor still has impacts on the results. Once the cell became saturated the uptake will not occur even if the incubation time is longer.

Using fluorescence microscopy, a qualitative analysis of the NPs fate inside the cells was performed (table 6). NPs appeared to be present in the cytoplasmatic compartment and did not apparently penetrate into the cell nucleus. However, 2D images dot not allow to differentiate between intracellular locations and surface-bound NPs. A 3D imaging using confocal microscopy should be performed to confirm these preliminary observations. These could also be linked to the toxicity results since NPs that enter the nuclear compartment can directly interact with the DNA molecule and are usually more genotoxic.

5.3.3 Cyto- and Genotoxicity of PMMA and PMMA-Eud NPs

From the best of our knowledge, there are very limited information about the cyto- and genotoxicity of PMMA and PMMA-Eud NPs. For this reason, the comparison of the data obtained in this study with that of other studies has been a difficult task. Using other articles and reported studies by indirect comparison can be another option to interpret our results.

5.3.3.1 Cytotoxicity Assessment

Early toxicity events are intimately connected to a dysfunctional mitochondria activity and the unbalanced production of ROS. Cell viability was explored considering the ability of mitochondrial dehydrogenases (oxidoreductases) to reduce the MTT. The effect of a short- and long-term exposure, 24 and 64 hours of incubation, was compared using the undifferentiated and differentiated MG-63 cell line (figure 24 and 25). The results indicated that none of the NPs was

toxic to “normal” MG-63 cells upon a short-term exposure. In contrast, for a longer exposure duration PMMA-Eud was cytotoxic and PMMA was only toxic at very high concentrations (2 and 5 mg/mL). Regarding the results of differentiated MG-63 cells, none of the tested formulations induced cytotoxic effects, irrespectively of the exposure duration. In a direct comparison between differentiated and undifferentiated MG-63 cells it is possible to assume that cellular responses are intimately linked to the specialization state of the tissues. This hypothesis is in agreement with the report of Gerlof et al (2013) about the cytotoxicity of ZnO and SiO_2 NPs in differentiated and undifferentiated Caco-2 cell lines. The authors found out that SiO_2 NPs only reduced the viability of undifferentiated cells. As for ZnO NPs, which are partially soluble, cytotoxic effects were observed in both cell lines, although a higher dose of particles was required to achieve toxic effects in dfifferentiated cells comparable to those observed in the undifferentiated line. In addition, Pradines et al (2015) also investigated the toxicity of poly(isobutylcyanoacrylate)-coated and uncoated NPs in three epithelial cell models: HeLa under undifferentiated state and Caco-2/TC7 and HT-29/MTX under differentiated states. The results showed lower cytotoxic effects in Caco-2/TC7 and HT-29/MTX when directly compared with HeLa cells that presented a strong toxic effect. Another outcome pointed out in that study was that surface-coated NPs with chitosan become less toxic than uncoated NPs. Taken together, these studies suggest that undifferentiated cell lines are more sensitive towards cytotoxic effects of different NPs (composition, size and surface charge) than the differentiated counterparts. On the other hand, the latter better mimic in vivo tissues due to their specialized geno- and phenotype. Thus, undifferentiated osteoblasts may represent a sensitive cell model for an initial screening of NPs toxicity, a valuable feature in pharmacological studies to explore the safer dose-range of a drug. Moreover, combining both cellular responses should represent a more accurate experimental system for a more comprehensive toxicological assessment of new NPs or drugs. In addition, an interesting option to reduce NPs toxicity will be to explore materials to coat NPs surfaces in order to make them more biocompatible as described by Pradines et al (2015).

Evaluation of the ROS production is a vital step for biosafety assessment of nanomaterials. The ability of NPs to induce ROS and, consequently, oxidative stress usually represents an early sign of cyto- and genotoxicity in cells. In fact, an overproduction of ROS can induce oxidative stress with repercussions in several organelles. Cells also have antioxidant mechanisms to protect themselves against the harmful effects of ROS, specially the genotoxic effects. These mechanisms are activated instantly when ROS are detected and, for that reason, the time-points explored in this work were 1 and 3 hours. The results (figure 26) showed that neither PMMA nor PMMA-Eud affects, in a significant way, the intracellular production of ROS in differentiated osteoblasts. These results agree with those reported by Graça (2014) showing that none of these NPs induced a significant ROS formation in MG-63 cultured under normal conditions (Annex 4). These negative results are also consistent with those obtained by the FPG-modified comet assay that assesses oxidized purines. Ciapetti et al (2000) reported a cytotoxicity study *in vitro*, using 10 PMMA-based bone cements in HL-60 cells. After 24 hours, two of the tested cements induced the production of ROS. However, the presence of other compounds

(BaSO4, hidorquinones, benzoylperoxide, etc) in their composition was also reported and their effects on ROS induction could not be excluded. Besides, the materials that are incorporated in bone cements are at the micro- or macroscale, and for that reason are not comparable to NPs behaviour. Several studies report the induction of free radicals of oxygen by NPs used in biomedical applications. Silica, TiO_2, and Metal NPs are examples of oxidative stress-inducing NPs. Metal NPs can also release metallic ions, e.g., Fe2+, Ag+, Cu+ ions that easily interact with cell components and induce ROS or bind to DNA bases (Magdolenova et al. 2014). Mehri *et al* (2012) found that polysaccharide cationic NPs were able to induce ROS in 16HBE14o- (humam bronchial cells), that was detected by the modified Comet assay with FPG. However, few studies reported ROS induction by polymeric NPs (Mehri et al 2012).

To summarize, PMMA and PMMA-Eud did not produce oxidative damage in differentiated osteoblasts exposure, confirming the previous negative effect obtained in undifferentiated cells. These results contribute to the indication that the NPs under study are safe, in terms of oxidative stress assessment.

5.3.3.2 Genotoxicity Assessment

The comet assay has proved to be a sensitive method to quantify DNA strand breaks and oxidative DNA lesions (Huk et al. 2015). In this work, by the analysis of two individual time-points of exposure, it was possible to detect differences in the DNA lesions induced by PMMA and PMMA-Eud NPs (figures 27 and 28). The shortest time-point, 3h, revealed more deleterious effects of both NPs formulation to undifferentiated osteoblasts. In fact, both NPs were able to induce strand breaks at the DNA level at all concentrations tested. The differences between the level of DNA lesions induced by PMMA-Eud and PMMA were not significant, even though the former was slightly more genotoxic. After 24 hours exposure, the level of DNA breaks induced by each NP was 30 to 40% lower than that measured at 3 hours suggesting that the sensitivity of the comet assay to detect the NPs-induced damage is higher at 3h. It can be argued that cells activate intrinsic repair mechanisms to reduce the genetic damage caused by the short-term exposure to NPs. This also means that some of the the induced lesions are reversible and do not constitute a permanent DNA damage event, at least for the lowest concentration tested.

A similar effect was described by El Yamani et al. (2016) for metallic NPs, indicating that using two time-points is crucial to detect the DNA damaging effects of NPs. The genotoxicity of these NPs have also been evaluated in a previous work and no genotoxicity was detected in L929 cells (murine fibrobasts) as assessed by the Comet assay (Graça 2014). These contradictory results suggest that different cell line may display different responses and favours the use of more than one cell line to assess the toxicity of NPs. The same observation came up from the study of Platel et al. (2015) who studied the potential genotoxic effects induced by polymeric NPs with different sizes and surface charges in three cell lines, being the results positive in one of the cell lines only. The authors also concluded that for the same cell line, NPs with positive surface charge

presented higher genotoxicity in the comet assay. In this study, both NPs were genotoxic in the comet assay and none of them became positively charged after dispersion in the cell culture medium (PMMA NPs are almost neutral and PMMA-Eud NPs are negatively charged in culture medium) although the pristine PMMA-Eud NP was positively charged. In respect to the uptake by cells, both NP formulations were rapidly internalized by MG63 cells, being PMMA more internalized than PMMA-Eud at the concentration of 0.1 mg/mL. PMMA-Eud were slightly more genotoxic than the former NP.

Another important feature that is often referred by several authors is the NPs propensity to form aggregates/agglomerates in the cell culture medium and how this behaviour influences their toxicity. Tarantini et al (2015) and Gerloff et al. (2013) related higher toxicity levels to the aggregates/agglomerates formation during the cytotoxic assessment. Authors found that the genotoxic effects of NPs are more likely to be mediated through oxidative stress rather than a direct interaction with the DNA structure. In this work, PMMA-Eud was more prone to form aggregates/agglomerates and revealed to be more slightly more genotoxic when compared to PMMA NPs. This can be related to NP-cell interactions that will trigger cell responses that indirectly result in DNA damage.

On the other hand, the addition of the FPG enzyme has been described as increasing the sensitivity of the assay given that it allows the detection of oxidised purines as DNA strand breaks. However, in this work no significant differences were observed in the results obtained with and without FPG treatment, indicating that these NPs do not induce oxidative DNA damage under the tested conditions. These findings agree with the negative results obtained for ROS production in this cell line and suggest that these NPs are not able to induce ROS formation. A similar finding was reported by Graça (2014) for the same NPs tested in murine fibroblasts and in undifferentiated MG-63 cell line, concluding that after 1 and 2 hours of exposure, neither PMMA, nor PMMA-Eud was able to induce ROS formation for both cell models tested (annex 4).

Finally, the response of differentiated MG-63 cells still needs to be explored to find out if the level of specialization of the cell model can reduce the harmful effects, similarly to what happened in the MTT assay.

The capacity of the PMMA and PMMA-Eud NPs to produce chromosome damage was appraised by the CBMN assay using differentiated and undifferentiated osteoblasts. This methodology provides an entire analysis of the cyto- and genotoxic effects of an agent. The assay detect if a specific compound is able to induce MNi formation, but is also used to identify if the damage was related to chromosome loss or breakage and thus, classify the agents with aneugenic or clastogenic activity, respectively (Fenech 2000). The results were all negative (figure 29, 30 and 31), i.e., neither PMMA nor PMMA-Eud were able to induce chromosome

damage. Taken together with the results of the comet assay these results indicate that PMMA and PMMA-Eud are able to affect the DNA stability and induce primary DNA lesions (comet assay) that are apparently repaired because no chromosome alterations were detected by the CBMN assay. In fact, DNA single strand breaks, if left unrepaired, may be converted in double strand breaks that, in turn, can give rise to chromosome breaks after DNA replication. However, if the single strand breaks are efficiently repaired by the cell repair machinery, no chromosome damage will be apparent (Pillco & Peña 2014) . On the other hand, in a previous study with L929 fibroblasts, an induction of MNi formation was observed following exposure to PMMA but not to PMMA-Eud (Santos 2015). Merhi *et. al* (2012) reported in CBMN assay genotoxic effects induced by polysaccharide NPs at the 16HBE14o cell line, but only for the highest concentrations studied. In fact, they observed ROS formation after the exposure that seems to generate lipid adducts and will have repercussive impacts on chromosome structures.

Regarding the cytotoxicity estimated by the CBPI and RI indexes, the undifferentiated osteoblasts were not significantly affected by the NPs treatment. However, cells cultured under differentiation conditions showed a significant increase in the CBPI value at 1 mg/mL and in the RI at 0.1 mg/mL and 1 mg/mL over the control, after exposure to PMMA NPs. These elevated indexes may suggest that PMMA NP are able to further stimulate cells to divide and to accelerate the cell cycle. These events may contribute to a tumor promoter activity that must be further explored. Nevertheless, in a previous study with these NPs (Santos, 2015), such effect was not reported for L929 fibroblasts. Kinase proteins are the main responsible for the regulation of cell cycle events and some NPs can disturb some checkpoints that will affect the whole process (Magdolenova et al. 2014).

Although the CBMN assay has been pointed as a sensitive assay to be used in nanotoxicology, due to de deposition of NPs over the cell structures, some results had been neglected since NPs deposits represent an obstacle to the analysis of the main nucleus and cell boundaries. This may represent a limitation of this assay. Moreover, concentrations range must be adapted concerning the uptake efficiency of the differentiated cells to improve the results.

In conclusion, the results of this study showed that PMMA and PMMA-Eud NPs are uptaken by osteoblasts and can exert some cytotoxic and genotoxic effects. PMMA-Eud was shown to induce cytotoxic effects in long-term exposures reducing cell viability. However, this outcome was not confirmed in the differentiated cell model. PMMA seemed to induce toxicity in human osteoblasts at very high concentrations only, irrespectively of the status of cell specialization. PMMA-Eud NPs formulation had a higher propensity to form aggregates/agglomerates, which may reduce their bioavailability and their internalisation efficiency; their tendency to adsorb to cells surface may contribute to the cytotoxicity noticed at 64 hours of exposure. Both NPs formulations impacted on the DNA integrity leading to genetic damage (detected by the Comet assay). Due to the fact that no chromosome structure alterations were distinguished by the CBMN assay, it may be argued that the induced damages are reversible

and do not constitute a permanent effect. The mechanism behind the observed genotoxicity is probably not mediated by oxidative stress since no effects were observed by the two different endpoints explored (H_2DCFDA assay and the modified Comet assay with FPG). Due to their large size it is not expected that these NPs can cross the nuclear envelop pores, which is in line with the absence of the NPs in the cell nucleus, as observed by fluorescence microscopy. Thus, a direct interaction of the NPs with DNA causing DNA breaks detectable by the comet assay is not probable to occur. Other mechanisms related to the cell homeostasis disruption caused by NPs persistence in the cytoplasm may have mediated the transient production of DNA breaks. The DNA repair systems seem not to be affected by the NPs, given that a decrease of the level of DNA lesions was detected between 3h and 24h exposure and no chromosome breaks that could have resulted from unrepaired DNA breaks were not observed.

6. Conclusions and Future Perspectives

New drug delivery systems are becoming an increasingly important field of pharmacology, where biomaterials can improve the pharmacodynamics and reduce the side effects of a drug. Due to their distinct properties, NPs are conveniently used as nanocarriers for drug delivery systems and may constitute an answer to deal with infections that are hard to treat and tend to locate in poorly irrigated tissues i.e. bone. Innovative products require safe-by-design approach, considering the potential risks associated with the introduction of these materials both to human health and the environment.

The main goal of this project was to perform a biosafety evaluation of novel nanocarriers, PMMA and PMMA-Eud, through the characterization of their cytotoxic and genotoxic potential in human osteoblasts, as the main target of these NPs in the human body. In respect to the NPs production and characterization, SESE represents an adequate method to obtain plain PMMA and PMMA-Eud with a size distribution of 500 nm. It was also found that cell culture conditions can highly affect NPs features and a physicochemical characterisation must always be performed with different dispersant mediums, mostly those that are able to mimic the in vitro conditions. Cell assays revealed that PMMA-Eud were slightly more cytotoxic than PMMA formulation, but these effects were highly reduced when the exposure occurred in differentiated MG-63 cell line that better mimic the bone tissue. On the other hand, both NPs induced genotoxic effects detected by the Comet assay, more pronounced after short-term exposures. However, those effects are possibly transient and reversible, since the chromosome integrity was not affected as assessed by the micronucleus assay. It should not be ignored that PMMA promote a slight stimulus on the cell cycle progression, an event that is usually associated to tumour promotor activity and that should be explored.

In this work and in the previous one, different cell models were used to explore the genotoxic effects to these NPs including fibroblasts (murine) and the human osteoblast MG-63 cell line cultured under normal and differentiation medium conditions. Despite the fact that L929 cell line constitutes a recommended model to perform cell studies (ISO 10993-5) (Graça 2014), the data obtained with MG-63 cell line constitute, for the purpose of this study, a more adequate and probably more sensitive cell model to explore the NPs effects, since MG-63 cells try to mimic the target tissue. In another perspective, it also demonstrated that different cell lines are needed for further investigation of the potential toxicological effects especially for NPs, since one cell model could not be sufficient to infer about the whole organism toxicity.

The potential effects of these NPs carriers using other endpoints or on cell lines representative of other tissues still need to be explored. The endpoints may refer to gene mutations or gene and protein expression, and to inflammatory markers In addition, the possible effects of PMMA acting like a stimulating agent of the cell cycle deserves further analysis.

Furthermore, an extrapolation to in vivo models constitute an important extension of this work and is essential not only to examine cyto- and genotoxic effects of both NPs in a more realistic perspective, but also to demonstrate the most relevant concentrations that the target tissue is exposed to, excluding false positives due to unrealistic dose-ranges that may be tested in vitro. Though different studies are still needed to confirm and demonstrate PMMA and PMMA-Eud nanocarriers biocompatibility and safety, they have already proved to be a promising alternative to the available conventional treatments to osteomyelitis and the safe-by-design approach has been followed.

7. References

American Type Culture Collection, 2011. MTT Cell Proliferation Assay Instruction Guide. Components, 6597, pp.1–6.

Arora, S., Rajwade, J.M. & Paknikar, K.M., 2012. Nanotoxicology and in vitro studies: The need of the hour. Toxicology and Applied Pharmacology, 258(2), pp.151–165.

Bettencourt, A et al., 2010. Incorporation of tocopherol acetate-containing particles in acrylic bone cement. Journal of microencapsulation, 27(6), pp.533–541.

Bettencourt, A. & Almeida, A.J., 2012. Poly(methyl methacrylate) particulate carriers in drug delivery. Journal of Microencapsulation, 29(4), pp.353–367.

Bettencourt, A. & Almeida, A.J., 2014. Poly(Methyl Methacrylate) (PMMA): Drug Delivery Applications. Encyclopedia of Biomedical Polymers and Polymeric Biomaterials, pp.6511–6525.

Bhattacharjee, S. & Brayden, D.J., 2015. Development of nanotoxicology : Implications for drug delivery and medical devices. Nanomedicine (Lond.), 10(14), pp.2289–2305.

Birt, M.C. et al., 2017. Osteomyelitis: Recent advances in pathophysiology and therapeutic strategies. Journal of Orthopaedics, 14(1), pp.45–52.

Boskey, A.L., 2013. Bone composition: relationship to bone fragility and antiosteoporotic drug effects. BoneKEy reports, 2(July), p.447.

Chin, L.K. et al., 2011. Production of reactive oxygen species in endothelial cells under different pulsatile shear stresses and glucose concentrations. Lab on a chip, 11(11), pp.1856–63.

Ciapetti, G. et al., 2000. Cytotoxic effect of bone cements in HL-60 cells: distinction between apoptosis and necrosis. Journal of biomedical materials research, 52(2), pp.338–45.

Clarke, B., 2008. Normal bone anatomy and physiology. Clinical journal of the American Society of Nephrology : CJASN, 3 Suppl 3, pp.131–139.

Collins, A R., 2004. The comet assay for DNA damage and repair: principles, applications, and limitations. Molecular Biotechnology, 26(3), pp.249–261.

Collins, A.R. et al., 2008. The comet assay: Topical issues. Mutagenesis, 23(3), pp.143–151.

D'Autréaux, B. & Toledano, M.B., 2007. ROS as signalling molecules: mechanisms that generate specificity in ROS homeostasis. Nature Reviews Molecular Cell Biology, 8(10), pp.813–824.

Das, S., Suresh, P.K. & Desmukh, R., 2010. Design of Eudragit RL 100 nanoparticles by nanoprecipitation method for ocular drug delivery. Nanomedicine: Nanotechnology, Biology, and Medicine, 6(2), pp.318–323

Davis, J.S., 2005. Management of bone and joint infections due to Staphylococcus aureus. Internal Medicine Journal, 35(79–96).

Dekkers, S. et al., 2016. Towards a nanospecific approach for risk assessment. Regulatory Toxicology and Pharmacology, 80, pp.46–59.

Donlan, R.M., 2001. Biofilm formation: a clinically relevant microbiological process. Clinical infectious diseases : an official publication of the Infectious Diseases Society of America, 33(8), pp.1387–1392.

Ducy, P., Schinke, T. & Karsenty, G., 2000. The osteoblast: a sophisticated fibroblast under central surveillance. Science (New York, N.Y.), 289(5484), pp.1501–1504.

Edmondson, R. et al., 2014. Three-dimensional cell culture systems and their applications in drug discovery and cell-based biosensors. Assay and drug development technologies, 12(4), pp.207–18.

Egerton, R.F., 2005. Physical Principles of Electron Microscopy, Springer US 1st edition pp.25-41.

El Yamani, N. et al., 2016. In vitro genotoxicity testing of four reference metal nanomaterials, titanium dioxide, zinc oxide, cerium oxide and silver: towards reliable hazard assessment. Mutagenesis, (5), p.60.

European-Scientific-Committee, 2009. Risk assessment of products of nanotechnologies.

Evans, S.J. et al., 2016. Critical review of the current and future challenges associated with advanced in vitro systems towards the study of nanoparticle (secondary) genotoxicity. Mutagenesis, (November 2016), pp.233–241.

Evonik, 2002. Setting benchmarks in oral solid dosage forms. Evonik Industries, pp.1-16.

Fenech, M. et al., 2003. Intra- and inter-laboratory variation in the scoring of micronuclei and nucleoplasmic bridges in binucleated human lymphocytes Results of an international slide-scoring exercise by the HUMN project. , 534, pp.45–64.

Fenech, M., 2000. The in vitro micronucleus technique. Mutation Research - Fundamental and Molecular Mechanisms of Mutagenesis, 455(1–2), pp.81–95.

Fenech, M., 2007. Cytokinesis-block micronucleus cytome assay. Nature Publishing Group, 2(5), pp.1084–1104.

Ferreira, I., 2015. Novel particulate antibiotic-loaded platforms as sustained drug delivery systems for bone infection treatment. Universidade de Lisboa pp.63-129.

Ferreira, I.S. et al., 2015. Improvement of the antibacterial activity of daptomycin-loaded polymeric microparticles by Eudragit RL 100: An assessment by isothermal microcalorimetry. International Journal of Pharmaceutics, 485(1–2), pp.171–182.

Fleischer, C.C. & Payne, C.K., 2014. Nanoparticle − Cell Interactions: Molecular Structure of the Protein Corona and Cellular Outcomes. Acc. Chem. Res., 47, pp.2651–2659.

Florindo, H.F. et al., 2010. Surface modified polymeric nanoparticles for immunisation against equine strangles. International Journal of Pharmaceutics, 390(1), pp.25–31.

Gatoo, M.A. et al., 2014. Physicochemical properties of nanomaterials: Implication in associated toxic manifestations. BioMed Research International, 2014.

Gerloff, K. et al., 2013. Influence of simulated gastrointestinal conditions on particle-induced cytotoxicity and interleukin-8 regulation in differentiated and undifferentiated Caco-2 cells. Nanotoxicology, 7(4), pp.353–66.

Gilbert S., 2000. Osteogenesis: The Development of Bones. Development Biology, Chapter 14 6th edition pp. 368-412.

Glei, M., Schneider, T. & Schlormann, W., 2016. Comet assay: an essential tool in toxicological research. Archives of Toxicology, 90(10), pp.2315–2336.

Goldberg, M., Langer, R. & Jia, X., 2011. Nanostructured materials for applications in drug delivery and tissue engineering. Journal of Biomater Sci Polym, 18(2), pp.241–268.

Gomes, D., Pereira, M. & Bettencourt, A.F., 2013. Osteomyelitis: An overview of antimicrobial therapy. Brazilian Journal of Pharmaceutical Sciences, 49(1), pp.13–27.

Grabowski, P., 2015. Physiology of bone. Calcium and Bone Disorders in Children and Adolescents: Second Edition, 28, pp.33–55.

Graça, D., 2014. Biological Effects of Acrylic Engineered Particulate-Systems. Faculdade de Ciências e Tecnologias - Universidade Nova de Lisboa pp. 3-63.

Held, P., 2012. An Introduction to Reactive Oxygen Species Measurement of ROS in Cells. BioTek Instruments, pp.1–14.

Hocherl, A. et al., 2012. Competitive Cellular Uptake of Nanoparticles Made From Polystyrene , Poly (methyl methacrylate), and Polylactide Anita Ho. Macromolecular Bioscience, pp.454–464.

Huk, A. et al., 2015. Critical factors to be considered when testing nanomaterials for genotoxicity with the comet assay. Mutagenesis, 30(1), pp.85–88.

ICH, 2011. Impurities: Guideline for Residual Solvents Q3C (R5). International Conference on Harmonization of Technical Requirements for Registration of Pharmaceuticals for Human Use, 44(October 2002), p.29.

Ingham, B. et al., 2011. How nanoparticles coalesce: An in situ study of Au nanoparticle aggregation and grain growth. Chemistry of Materials, 23(14), pp.3312–3317.

Iu, M.F. et al., 2005. Dexamethasone suppresses Smad3 pathway in osteoblastic cells. Journal of Endocrinology, 185(1), pp.131–138.

Jayakumar, Prakash, Silvio, L. Di, 2010. Osteoblasts in bone tissue engineering Osteoblasts in bone tissue engineering. Journal of engineering in Medicine 224(12) pp. 1415-1417.

Jiang, X. & Gao, H., 2017. Neurotoxicity of Nanomaterials and Nanomedicine, Elsevier Inc Chapter 4, pp. 75-98.

Klabunde, R., 2009. Nanoscale Materials in Chemistry 2nd Edition., John Wiley & Sons, Inc Chapter 1, pp. 1-13.

Knott, G. & Genoud, C., 2013. Is EM dead? Journal of Cell Science, 126(20), pp.4545–4552.

Kong, I., 2015. Design and Applications of Nanostructured Polymer Blends and Nanocomposite Systems. Elsevier Inc Chapter 7, pp. 125-154

Langenbach, F. et al., 2013. Effects of dexamethasone, ascorbic acid and β-glycerophosphate on the osteogenic differentiation of stem cells in vitro. Stem Cell Research & Therapy, 4(5), p.117.

Lew, D.P. & Waldvogel, F.A., 2004. Osteomyelitis. Lancet, 364(1474–547X (Electronic)), pp.369–379.

Louro, H. et al., 2015. Role of Nanogenotoxicology Studies in Safety Evaluation of Nanomaterials. In Nanotechnology applications for tissue engineering. Elsevier Inc Chapter 16, pp. 263-283.

Magdolenova, Z. et al., 2014. Mechanisms of genotoxicity. A review of in vitro and in vivo studies with engineered nanoparticles. Nanotoxicology, 8(July 2016), pp.233–78.

Malvern Instruments Ltd, 2007. Mastersizer 2000 User Manual. p.154.

Malvern instruments, 2004. Zetasizer Nano Series User Manual. Department of Biochemistry Biophysics Facility , University of Chambridge, (2), p.207.

Mascio, C.T.M., Alder, J.D. & Silverman, J.A., 2007. Bactericidal action of daptomycin against stationary-phase and nondividing Staphylococcus aureus cells. Antimicrobial Agents and Chemotherapy, 51(12), pp.4255–4260.

Merhi, M. et al., 2012. Study of serum interaction with a cationic nanoparticle: Implications for in vitro endocytosis, cytotoxicity and genotoxicity. International Journal of Pharmaceutics, 423(1), pp.37–44.

Murugan, R. & Ramakrishna, S., 2005. Development of nanocomposites for bone grafting. Composites Science and Technology, 65(15–16 SPEC. ISS.), pp.2385–2406.

Nel, A.E. et al., 2009. Understanding biophysicochemical interactions at the nano–bio interface. Nature Publishing Group, 8(7), pp.543–557.

Oberdörster, G., 2010. Safety assessment for nanotechnology and nanomedicine: Concepts of nanotoxicology. Journal of Internal Medicine, 267(1), pp.89–105.

OECD Guidlines, 487, 2010. Guideline for the testing of chemicals: Invitro mammalian cell micronucleus test. *In Vitro*, (Accessed in July, 2016).

OECD Guidelines, 489, 2014. Guidelines for the Testing of Chemicals *In Vivo* Mammalian Alkaline Comet Assay, (Accessed in September, 2016).

Park, J.B., 2012. The effects of dexamethasone, ascorbic acid, and β-glycerophosphate on osteoblastic differentiation by regulating estrogen receptor and osteopontin expression. Journal of Surgical Research, 173(1), pp.99–104.

Pauksch, L. et al., 2014. In vitro assessment of nanosilver-functionalized PMMA bone cement on primary human mesenchymal stem cells and osteoblasts. PLoS ONE, 9(12), pp.1–19.

Pillco, A. & Peña, E. De, 2014. Genotoxicity and DNA Repair, Humana Press Chapter 3, pp. 43-57.

Platel, A. et al., 2015. Influence of the surface charge of PLGA nanoparticles on their in vitro genotoxicity, cytotoxicity, ROS production and endocytosis. Journal of Applied Toxicology, 36(3), pp.434–444.

Pradines, B. et al., 2015. Cell line-dependent cytotoxicity of poly(isobutylcyanoacrylate) nanoparticles coated with chitosan and thiolated chitosan: Insights from cultured human epithelial HeLa, Caco2/TC7 and HT-29/MTX cells. International Journal of Pharmaceutics, 491(1–2), pp.17–20.

Rassoolzadeh, H. et al., 2016. Overexpression of the scaffold WD40 protein WRAP53β enhances the repair of and cell survival from DNA double-strand breaks. Cell death & disease, 7(6), p.e2267.

Rauscher, H. et al., 2015. JRC SCIENCE FOR POLICY REPORT Towards a review of the EC Recommendation for a definition of the term " nanomaterial ".

Ravi, M. et al., 2015. 3D cell culture systems: Advantages and applications. Journal of Cellular Physiology, 230(1), pp.16–26.

Sanchez, F. & Sobolev, K., 2010. Nanotechnology in concrete - A review. Construction and Building Materials, 24(11), pp.2060–2071.

Santos, J., 2015. Nanotoxicology : study of nanomaterials genotoxic effects in cell lines. Universidade de Lisboa pp. 33-46.

Santos, J.G.F. et al., 2011. Production of bone cement composites: Effect of fillers, co-monomer and particles properties. Brazilian Journal of Chemical Engineering, 28(2), pp.229–241.

Shiga, M. et al., 2003. Ascorbic acid induces collagenase-1 in human periodontal ligament cells but not in MC3T3-E1 osteoblast-like cells: potential association between collagenase expression and changes in alkaline phosphatase phenotype. Journal of bone and mineral research : the official journal of the American Society for Bone and Mineral Research, 18(1), pp.67–77.

Singh, R.P. & Ramarao, P., 2013. Accumulated polymer degradation products as effector molecules in cytotoxicity of polymeric nanoparticles. Toxicological Sciences, 136(1), pp.131–143.

Sittampalam, G.S. et al., 2016. In Vitro Biochemical Assays. In Assay and drug development technologies. Eli Lilly & Company and the National Center for Advancing Translational Sciences Bethesda, Chapter 3 pp. 87-96.

Sokolov, S. V. et al., 2015. Reversible or Not? Distinguishing Agglomeration and Aggregation at the Nanoscale. Analytical Chemistry, 87(19), pp.10033–10039.

Sutariya, V.B. & Pathak, Y., 2015. Biointeractions of Nanomaterials. CRC Press pp. 30-382

Tarantini, A. et al., 2015. Toxicity, genotoxicity and proinflammatory effects of amorphous nanosilica in the human intestinal Caco-2 cell line. Toxicology in Vitro, 29(2), pp.398–407.

Thakral, S., Thakral, N. & Majumdar, D., 2013. Eudragit®: a technology evaluation. Expert Opinion on Drug Delivery, 10(1), pp.131–149.

Vandghanooni, S. & Eskandani, M., 2011. Comet assay: A method to evaluate genotoxicity of nano-drug delivery system. BioImpacts, 1(2), pp.87–97.

Vauthier, C. & Bouchemal, K., 2009. Methods for the Preparation and Manufacture of Polymeric Nanoparticles. Pharmaceutical Research, 26(5), pp.1025–1058.

Veerachamy, S. et al., 2014. Bacterial adherence and biofilm formation on medical implants: a review. Proceedings of the Institution of Mechanical Engineers. Part H, Journal of engineering in medicine, 228(10), pp.1083–99.

Veronese, F.M. & Pasut, G., 2005. PEGylation, successful approach to drug delivery REVIEWS. Drug Discovery Today, 10(21), pp.1451–1458.

Vranic, S. et al., 2013. Deciphering the mechanisms of cellular uptake of engineered nanoparticles by accurate evaluation of internalization using imaging flow cytometry. Particle and fibre toxicology, 10:2, pp. 1-10.

Wagner, V. et al., 2006. The emerging nanomedicine landscape. 24(10), pp.1211–1217.

Walker, J.M., 2011. Cancer Cell Culture.Springer Berlin 2nd edition Chapter 15 pp. 219-255.

8. Annexes

Annex 1: Normalization assays with BSA protein

Results from calibration curves used in AP assay, Alizarin-red assay, and uptake assay, respectively.

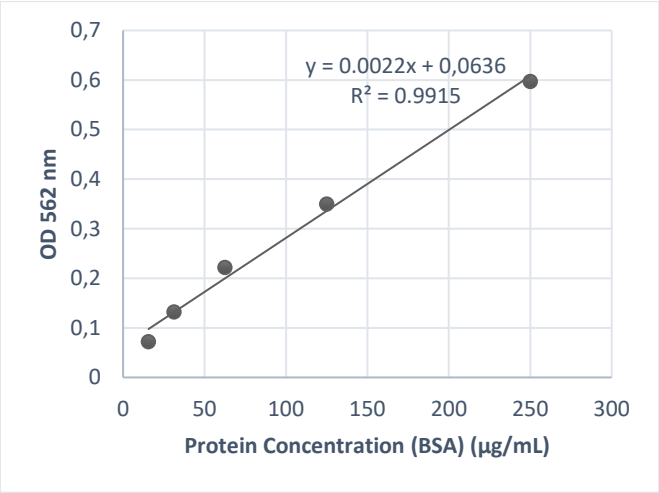

Figure A: Calibration curve using the BSA protein by the BCA method. The total amount of AP present in the lysates were calculated considering this assay.

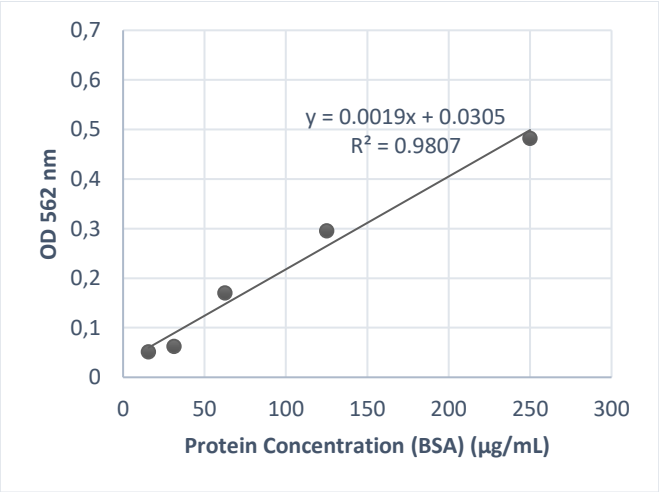

Figure B: Calibration curve using the BSA protein by the BCA method. The amount of calcium deposition present in the cells was calculated considering this assay.

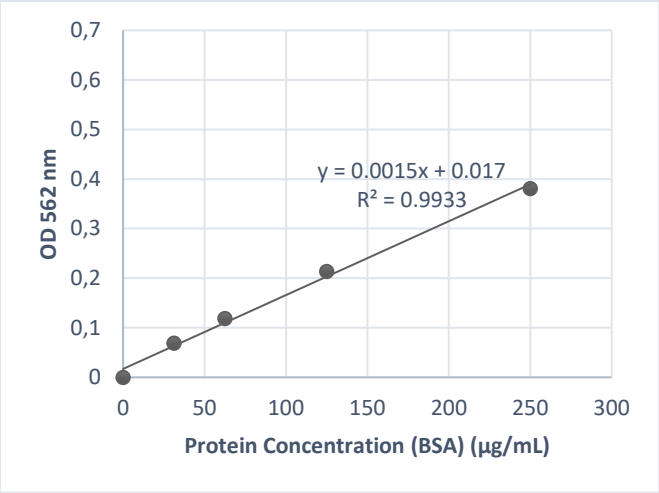

Figure C: Calibration curve using BSA protein by the BCA method. The amount of internalised NPs were calculated considering this assay.

Annex 2: Results of cytotoxicity assays

Results obtained in cytotoxicity assays are displayed considering the viability and the ROS detection, respectively.

Table A: MTT assay for undifferentiated MG-63 cell line.

	Cell viability (%) (Mean ± SD)			
	24 hours of incubation		64 hours of incubation	
NPs concentration	PMMA	PMMA-Eud	PMMA	PMMA-Eud
0	100 ± 0	100 ± 0	100 ± 0	100 ± 0
0.1	97.4 ± 9.3	107.7 ± 9	96.3 ± 3.9	83.0 ± 7.6
0.5	94.4 ± 5.9	111.4 ± 2.5	94.8± 2.9	75.0 ± 5.1
1	96.2 ± 13.0	101.7 ± 8.9	92.7 ± 2.4	66.2 ± 1.2
2	94.0 ± 3.0	107.5 ± 12.6	86.9 ± 0.7	59.0 ± 1.4
5	85.1 ± 3.0	101.5± 16.0	78.4 ± 4.5	52.1 ± 3.6
SDS (0.07%)	3.1 ± 0.3	1.5 ± 0.1	2.0 ± 0.7	1.4 ± 0.5

Table B: MTT assay for differentiated MG-63 cell line.

	Cell viability (%) (Mean ± SD)			
	24 hours of incubation		64 hours of incubation	
NPs concentration	PMMA	PMMA-Eud	PMMA	PMMA-Eud
0	100 ± 0	100 ± 0	100 ± 0	100 ± 0
0.05	90.5 ± 11.1	97.9 ± 12.6	96.5 ± 14.9	98.7 ± 4.8
0.1	89.3 ± 6.2	91.7 ± 15.3	104.4 ± 14.5	87.1 ± 16.2
0.5	84.3 ± 17.4	98.1 ± 12.6	101.0 ± 13.4	86.8 ± 19.2
1	85.9 ± 15.2	104.6 ± 14.3	89.9 ± 10.8	85.3 ± 17.4
2	81.6 ± 13.5	101.6 ± 14.4	100.3 ± 25.3	78.8 ± 17.4
SDS (0.07%)	1.3 ± 0.3	1.8 ± 0.5	1.6 ± 0.4	1.4 ± 0.1

Table C: ROS production for differentiated MG-63 cell line

	RFU (%) (Mean ± SD)			
	1 hour of incubation		3 hours of incubation	
NPs concentration	PMMA	PMMA-Eud	PMMA	PMMA-Eud
0	100 ± 0.0	100 ± 0.0	100 ± 0.0	100 ± 0.0
0.1	99.8 ± 10.8	102.7 ± 10.1	86.0 ± 6.8	100.4 ± 12.1
0.5	100.2 ± 5.7	87.3 ± 5.6	90.8 ± 8.5	104.7 ± 7.2
1	99.3 ± 3.9	93.2 ± 7.7	93.4 ± 10.7	102.1 ± 3.0
2	108.0 ± 8.5	94.9 ± 9.1	99.0 ± 5.0	103.3 ± 6.7
H_2O_2	8965.1 ± 570.1	9110.6 ± 492.5	8339.2 ± 506.0	8803.2 ± 552.6

Annex 3: Results of genotoxicity assays

Results obtained in the genotoxicity assays are displayed conserving the comet assay and the CBMN assay (micronucleus scores, CBPI and RI index)

Table A: Comet assay for undifferentiated MG-63 cell line after 3 hours of incubation. "N.P."- Not Performed.

	DNA in tail (%) (Mean ± SD)			
	PMMA		PMMA-Eud	
NPs concentration	Without FPG	With FPG	Without FPG	With FPG
0	4.0 ± 0.7	5.1 ± 1.0	6.3 ± 0.6	7.1 ± 0.2
0.1	9.5 ± 1.1	9.6 ± 2.4	12.3 ± 1.9	10.9 ± 1.0
0.5	12.7 ± 1.0	13.7 ± 1.4	14.2 ± 1.0	13.9 ± 1.6
1	13.4 ± 2.8	14.4 ± 1.0	15.6 ± 1.8	16.5 ± 1.3
2	14.2 ± 2.3	15.2 ± 2.2	17.4 ± 1.5	19.4 ± 3.6
5	14.8 ± 0.7	16.4 ± 3.4	N.P.	N.P.
E.M.S	32.2 ± 2.5	41.3 ± 2.7	37.3 ± 6.0	45.7 ± 6.7

Table B: Comet assay for undifferentiated MG-63 cell line after 24 hours of incubation. "N.P."- Not Performed.

	DNA in tail (%) (Mean ± SD)			
	PMMA		PMMA-Eud	
NPs concentration	Without FPG	With FPG	Without FPG	With FPG
0	4.1 ± 0.6	6.0 ± 0.6	4.0 ± 1.1	5.8 ± 1.9
0.1	6.4 ± 1.3	8.9 ± 1.3	6.4 ± 0.8	8.7 ± 2.8
0.5	8.9 ± 1.5	10.2 ± 1.6	8.5 ± 2.7	10.5 ± 2.7
1	9.0 ± 2.0	8.3 ± 2.6	9.3 ± 2.3	12.8 ± 4.7
2	9.7 ± 1.5	10.0 ± 0.9	12.0 ± 2.7	12.3 ± 1.3
5	10.7 ± 0.8	13.2 ± 1.0	N.P.	N.P.
E.M.S	21.4 ± 2.5	31.4 ± 3.8	29.6 ± 3.9	34.2 ± 5.3

Table C: Reduction (%) between the obtained values of DNA breaks between 3 and 24 hours of incubation without FPG. "N.P."- Not Performed.

	Reduction of the DNA in tail (%) between the 2 time-points	
	Without FPG	
NPs concentration	PMMA	PMMA-Eud
0.1	32.6	48.0
0.5	29.9	40.1
1	32.8	40.4
2	31.7	31.0
5	27.7	N.P

Table D: MNi scores for differentiated and undifferentiated MG-63 cell models. "N.P."- Not Performed.

	Undifferentiated MG-63		**Differentiated MG-63**	
	MNBNC/1000 BNC (Mean ± SD)		MNBNC/1000 BNC (Mean ± SD)	
NPs concentration	PMMA	PMMA-Eud	PMMA	PMMA-Eud
0	3.3 ± 0.5	3.5 ± 1.3	3.8 ± 1.3	3.8 ± 1.0
0.05	4.0 ± 0.8	3.0 ± 0.8	3.3 ± 1.0	3.3 ± 0.5
0.1	3.5 ± 1.0	3.8 ± 1.3	3.5 ± 1.3	4.0 ± 0.8
0.5	4.0 ± 0.8	2.3 ± 1.3	3.5 ± 1.0	4.8 ± 0.5
1	4.0 ± 1.4	1.8 ± 1.0	2.8 ± 0.5	5.0 ± 0.8
2	4.0 ± 2.4	2.8 ± 0.5	4.75 ± 1.5	6.0 ± 0.8
5	4.3 ± 0.5	1.5 ± 0.6	N.P.	N.P
MMC	13.5 ± 1.9	19.3 ± 2.6	17.8 ± 1.5	20.5 ± 1.3

Table E: CBPI and RI index for undifferentiated MG-63 cell line.

	CBPI (Mean ± SD)		**RI (%) (Mean ± SD)**	
NPs concentration	PMMA	PMMA-Eud	PMMA	PMMA-Eud
0	1.8 ± 0.0	1.8 ± 0.0	100 ± 0.0	100 ± 0.0
0.05	1.8 ± 0.2	1.7 ± 0.1	89.3 ± 0.4	92.9 ± 4.03
0.1	1.9 ± 0.1	1.9 ± 0.0	103.6 ± 0.0	105.5 ± 1.6
0.5	1.9 ± 0.0	1.8 ± 0.3	106.8 ± 0.6	101.0 ± 1.0
1	1.9 ± 0.2	1.9 ± 0.0	107.9 ± 3.0	105.5 ± 2.4
2	1.9 ± 0.1	2.0 ± 0.1	104.5 ± 0.2	107.4 ± 7.4
5	1.9 ± 0.1	1.8 ± 0.2	103.5 ± 1.1	101.3 ± 2.2
MMC	1.6 ± 0.1	1.6 ± 0.1	77.5 ± 0.8	73.9 ± 2.0

Table F: CBPI and RI index for differentiated MG-63 cell line

	CBPI (Mean ± SD)		**RI (%) (Mean ± SD)**	
NPs concentration	PMMA	PMMA-Eud	PMMA	PMMA-Eud
0	1.9 ± 0.0	1.8 ± 0.0	100 ± 0.0	100 ± 0.0
0.05	2.0 ± 0.0	1.8 ± 0.1	109.1 ± 4.6	93.2 ± 2.9
0.1	2.0 ± 0.1	1.7 ± 0.1	110.6 ± 1.1	90.2 ± 7.1
0.5	1.9 ± 0.0	1.8 ± 0.2	117.7 ± 3.0	95.1 ± 1.2
1	2.1 ± 0.0	1.9 ± 0.0	118. ± 0.8	102.1 ± 3.0
2	2.0 ± 0.1	1.7 ± 0.1	104.5 ± 2.0	85.3 ± 7.3
MMC	1.6 ± 0.1	1.4 ± 0.1	71.1 ± 1.5	50.8 ± 2.0

Annex 4: Supplementary material

During the thesis is often referred a previous work performed by Graça (2014). In this section, will be presented supplementary data obtained by the author to allow a better understanding of the results.

Table A: Yield of production per particle type (n=3) by Graça, 2014.

Particles	YP (%, *w/w*)
PMMAp	92.31 ± 15.38
PMMA-EUDp	32.43 ± 0.15

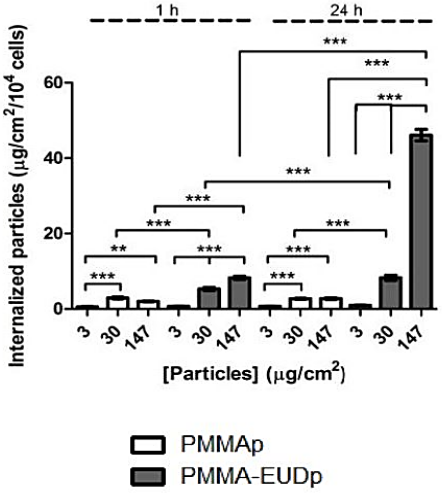

*Figure A: Results from the uptake assay in MG-63 cells, after particle exposure for 1 and 24 hours for undifferentiated MG-63 cells; Note - *, ** and *** correspond to p<0.05, p<0.01 and p<0.001, respectively (n=5) by Graça, 2014.*

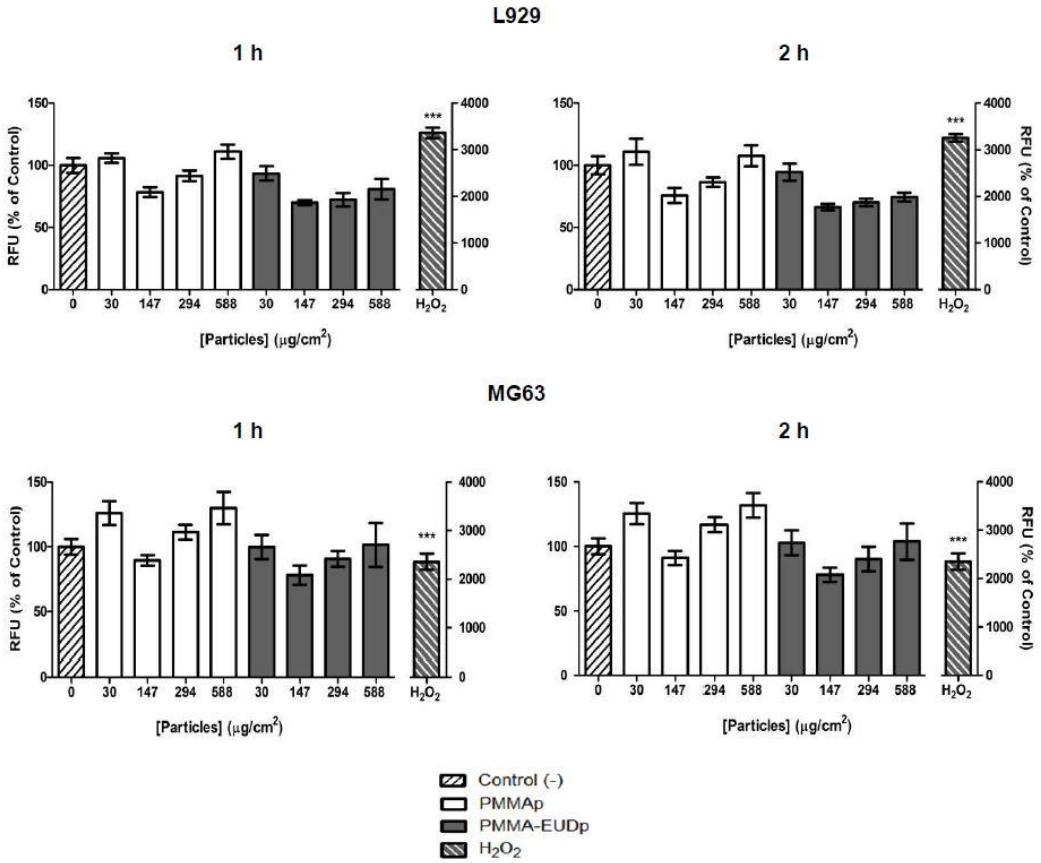

*Figure B: Evaluation on the formation of ROS through relative fluorescence unit percentage in L929 cell line and in undifferentiated MG-63 cells; Note - *** significantly different from control (culture medium) (p<0.001) by Graça, 2014.*

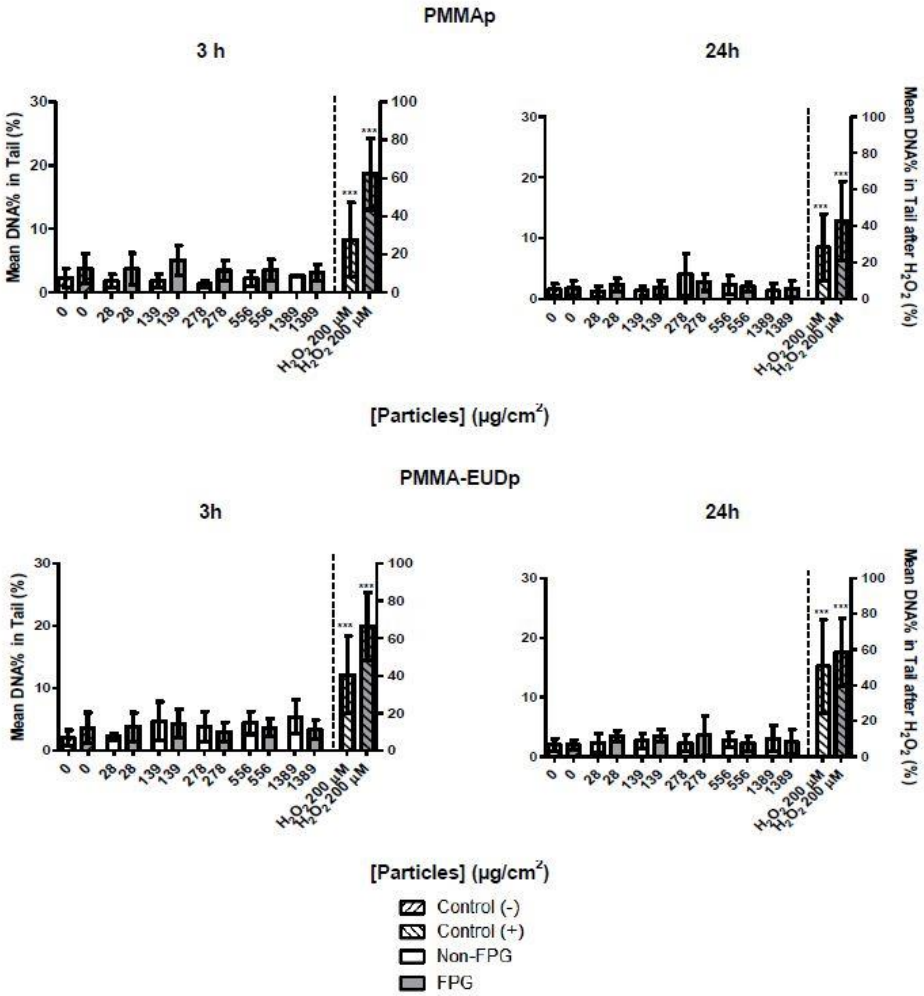

*Figure C: Results of comet assay obtained by Graça (2014) in L929 cell line. Note:*** significantly different from negative control (p<0.001).*